RESEARCH PAPER

Synthesis, Characterization, and In-Vivo Anti-Inflammatory Assessment of Novel Heterocyclic Derivatives..

Shabeena Parveen[1], Dr. Milind Sharad Pande[1]*, Dr. Sanjay J. Ingale[1]

[1]*Department of Pharmaceutical Sciences, IIMT University, Meerut, UP.*

ABSTRACT

The present study reports the design, synthesis, molecular docking, characterization, and in vivo anti-inflammatory evaluation of benzimidazole and isoxazole-based heterocyclic derivatives. A series of compounds was synthesized through optimized reaction schemes and structurally confirmed using IR, NMR, and mass spectrometry. Molecular docking studies against phospholipase A2 (PDB ID: 1Q7A) revealed that several derivatives represented strong binding affinities, surpassing the reference drug (Diclofenac). Among all screened molecules, the six compounds (MB3, FB5, BT4, CD4, CD16, and CD22) demonstrated the most favourable interaction profiles, supported by multiple hydrogen-bond and hydrophobic interactions within the active site. The in-vivo anti-inflammatory activity was assessed using the carrageenan-induced paw edema model in albino rats. Compounds FB5 and CD16 exhibited the highest percentage inhibition of edema (27.01% and 25.45% at 5 hours), closely approaching the standard drug (diclofenac-30.49%). Moderate activity was observed for MB3, BT4, CD4 and CD22. The histopathological analysis further confirmed a substantial reduction in inflammatory cell infiltration in treated groups...

Keywords: Benzimidazole derivatives, isoxazole derivatives, molecular docking, anti-inflammatory activity, carrageenan-induced paw edema

How to cite this article: Parveen S, Pande MS, Ingale SJ., Synthesis, Characterization, and In-Vivo Anti-Inflammatory Assessment of Novel Heterocyclic Derivatives....Int J Drug Deliv Technol. 2026;16(1s): 462-493; DOI: 10.25258/ijddt.16. 462-493

Source of support: Nil.

Conflict of interest: None

INTRODUCTION

Edema, erythema (redness), warmth, discomfort, and loss of function (stiffness and immobility) are among the more common signs and symptoms that the ancient medical term "inflammation" originally referred to. Currently, inflammation is defined as a series of fluctuating responses to tissue harm produced by toxic substances, environmental agents, trauma, overuse, or infection. As in many chronic disease conditions, some of these reactions can aid in wound healing, infection management, or pathology. A second line of defense against infectious pathogens is inflammation. A vital aspect of disease is the reactions triggered by inflammation. The suffixitis is used to describe diseases in which inflammation is the primary pathogenic feature. The immune system's humoral and cell-mediated reactions are essential to inflammation [1].

Changes in blood flow, an increase in blood vessel permeability, fluid movement, proteins, and white blood cells (leukocytes) from the circulatory system to the location of the damaged tissue are all possible outcomes of the inflammatory process. Acute inflammation occurs when the inflammatory reaction lasts only a few days; chronic inflammation, on the other hand, can result in organ failure, physiological degradation, and ultimately even death [2].

A highly coordinated network of several cell types is involved in the inflammatory response. Local reactions to tissue injury and infection are mediated by activated macrophages, monocytes, and other cells. In addition to chemokines and growth factors that attract neutrophils and monocytes to tissue injury sites, damaged epithelium and endothelial cells produce substances that initiate the inflammatory cascade. Neutrophils are the first cells attracted to an injury site, followed by monocytes, lymphocytes (natural killer cells - NK cells, B cells and T cells), and mast cells. Monocytes can differentiate into macrophages and dendritic cells, which are then recruited to damaged tissues by chemotaxis. Asthma, cancer, chronic inflammatory disorders, atherosclerosis, diabetes, and autoimmune and degenerative diseases are all associated with immune cell changes caused by inflammation [3].

Current anti-inflammatory medications, such as NSAIDs and corticosteroids, provide quick relief but have significant limits. NSAIDs inhibit COX enzymes, lowering prostaglandins that protect the GI tract, resulting in ulcers, bleeding, perforation, and cardiovascular problems such as hypertension, heart failure, and myocardial infarction, particularly with COX-2 inhibitors. Corticosteroids, while effective for acute inflammation, cause long-term problems at dosages greater than 40 mg/day prednisone equivalent (>3 months): recurrent infections, skin atrophy, avascular necrosis, osteoporosis, diabetes, psychological disorders, and GI bleeding, with risks increasing after 430 mg cumulative dose. Mitigation requires minimal dose, monitoring, and adjuncts such as calcium [4].

Heterocyclic compounds have received a lot of interest due to their numerous important medical and biological applications. Because of their wide synthetic study and functional application, research interest in heterocyclic molecules is quickly growing. They are present in more than 90% of innovative medications and bridge the gap between biology and chemistry, where much scientific discovery and application takes place. Heterocycles have

**Author for Correspondence: dean_pharma@iimtindia.net, shabena.pharma@gmail.com.*

applications in a variety of domains, including pharmaceutical chemistry, biochemistry and others. The primary applications of heterocyclic compounds are pharmaceuticals, agrochemicals and veterinary products [5].

Scaffolds are implants that are frequently used to deliver cells, medicines and genes into the body. Their uniform porosity structure provides the necessary support for cell adhesion, proliferation, differentiation, and migration. Leaching, freeze-drying, supercritical fluid technology, thermally induced phase separation, rapid prototyping, powder compaction, sol-gel, and melt molding are all techniques for fabricating a scaffold. Gene delivery from the scaffold is a diverse way to alter the environment and manage cell function. Scaffolds can be employed in a variety of tissue engineering applications, including bone formation, periodontal regeneration, cartilage growth, artificial corneas, heart valves, tendon repair, and ligament replacement. They are useful in cancer treatment, inflammation, diabetes, heart disease, and wound dressings. Scaffolds give a platform to extend the distribution of pharmaceuticals and genetic materials at a controlled time frame, as well as potentially being utilized to prevent infection following surgery and other chronic conditions, provided that they can be developed with appropriate medicines [6].

Heterocyclic compounds are essential in drug discovery, accounting for around 80% of pharmaceuticals. Benzimidazole, in particular, appears as an important aromatic heterocyclic system found in natural substances, with a vital significance in medicinal chemistry. Beyond its pharmaceutical significance, benzimidazole displays versatility in a variety of areas, including materials science and a wide range of pharmacological uses, including antiviral, antifungal, antioxidant, and anticancer activities. The importance of benzimidazole in both biological and industrial applications emphasizes its critical role as a flexible heterocyclic scaffold. Its exceptional characteristics, such as increased bioavailability, stability, and biological activity, have received significant interest from both researchers and industries [7].

Isoxazoles are five-membered aromatic heterocyclic compounds containing oxygen and nitrogen atoms at positions 1 and 2 of the ring structure. Isoxazole derivatives play an important role because of their varied biological actions, which include antibacterial, antiviral, antifungal, antitubercular, anti-diabetic, anti-epileptic, anticancer, antioxidant, anthelmintic, antipsychotic, analgesic, antimalarial, and anti-inflammatory properties. The isoxazole scaffold is found in a variety of medicinal compounds, including leflunomide (antirheumatic), zonisamide (anticonvulsant) and valdecoxib (nonsteroidal anti-inflammatory medication). Similarly, isoxazole derivatives like isocarboxazid function as monoamine oxidase inhibitors. It is used to treat depressive symptoms such as anxiety, panic attacks, and phobias. Isoxazole derivatives, such as sulfisoxazole, sulfamethoxazole, and oxacillin, are used in medical procedures to treat bacterial infections. Isoxazole pharmacophore is found in β-lactamase resistant antibiotics such dicloxacillin, cloxacillin, and flucloxacillin. Cycloserine is a naturally occurring antibiotic that possesses the isoxazole moiety with antitubercular effect [8].

The rational design of hybrid compounds integrating two bioactive heterocyclic frameworks has emerged as an efficient technique for increasing pharmacological activity while minimizing side effects. In this context, the benzimidazole and isoxazole moieties showed higher anti-inflammatory activity. Structural alteration with appropriate substitutions can further optimize physicochemical attributes, target selectivity, and biological performance [9, 10].

In this research work, we discuss the design, synthesis and molecular docking analysis of novel benzimidazole and isoxazole based derivatives, followed by extensive spectral characterization utilizing a variety of methods. The synthesized compounds were tested for in-vivo anti-inflammatory activity using known animal models to determine their therapeutic potential and safety. This study aims to find promising lead molecules that may act as effective anti-inflammatory agent and contribute to the development of safer alternatives for existing therapies.

2. MATERIALS AND METHODS

2.1 Chemicals and Reagents

Analytical-grade reagents and solvents were used for synthesis. Albino rats (either sex) were obtained from an approved animal facility under project proposal no. RVN1/1AEC/24-25/15 and acclimatized under standard laboratory conditions.

2.2 General Scheme for Heterocyclic Derivatives

2.2.1 General Scheme for Benzimidazole Based Derivatives

To a solution of OPDA (5.75 g, 50mmol) and phenylglycine (4.77g, 50mmol) in 4N HCl (100 mL) was refluxed for 4-6 hours to get compound A**.** Next, the reaction mixture was further stirred for 1 h at 70 °C. After that, compound A in acetic medium of acetic acid was refluxed with substituted phthalic anhydrides to get compound B in good to excellent yield. The progress of reaction was monitored by TLC using Toluene: Ethyl acetate: Formic acid 5:4:1 as mobile phase. The solid precipitate was filter out as well as re-crystalized with ethanol [11-14].

Benzimidazole Scheme

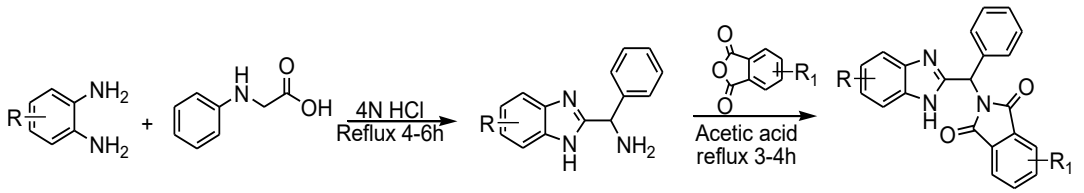

Phenylglycine | Compound A | Compound B

R= H,CH_3,Cl and F

R_1= H,NO_2, Br, COOH and F

R=H and R_1=H, NO_2, Br, COOH and F

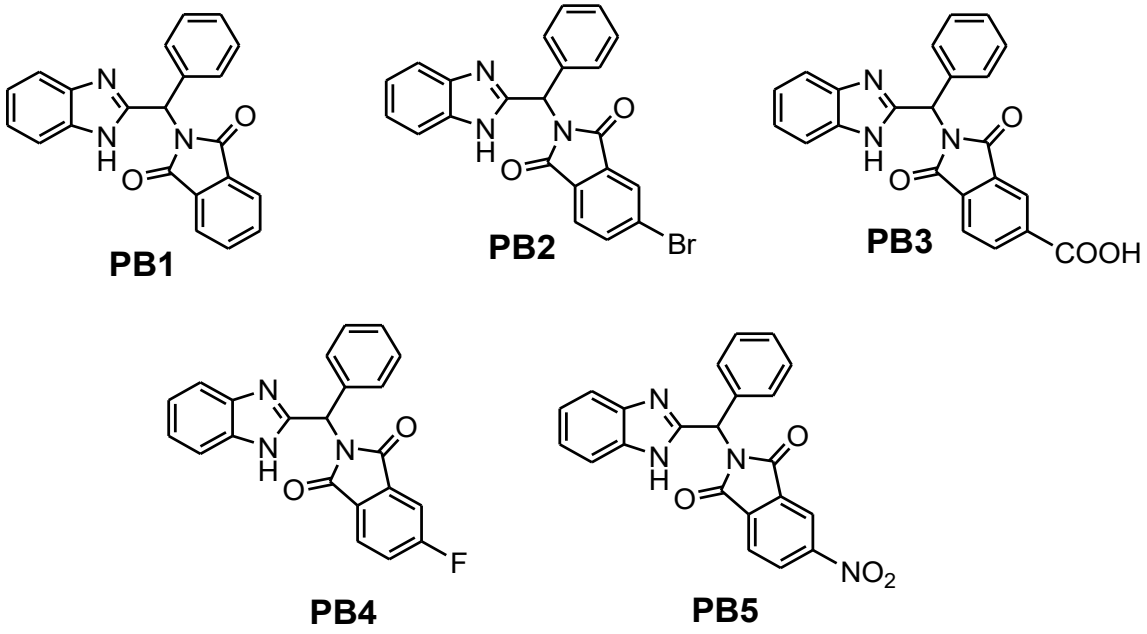

R=CH_3 and R_1=H, NO2, Br, COOH and F

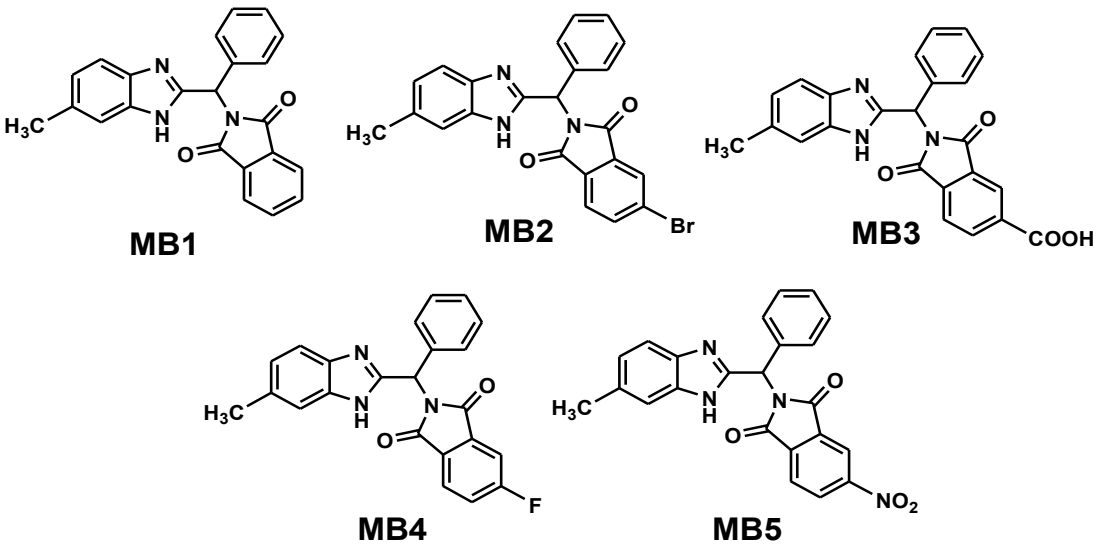

*Author for Correspondence: dean_pharma@iimtindia.net, shabena.pharma@gmail.com.

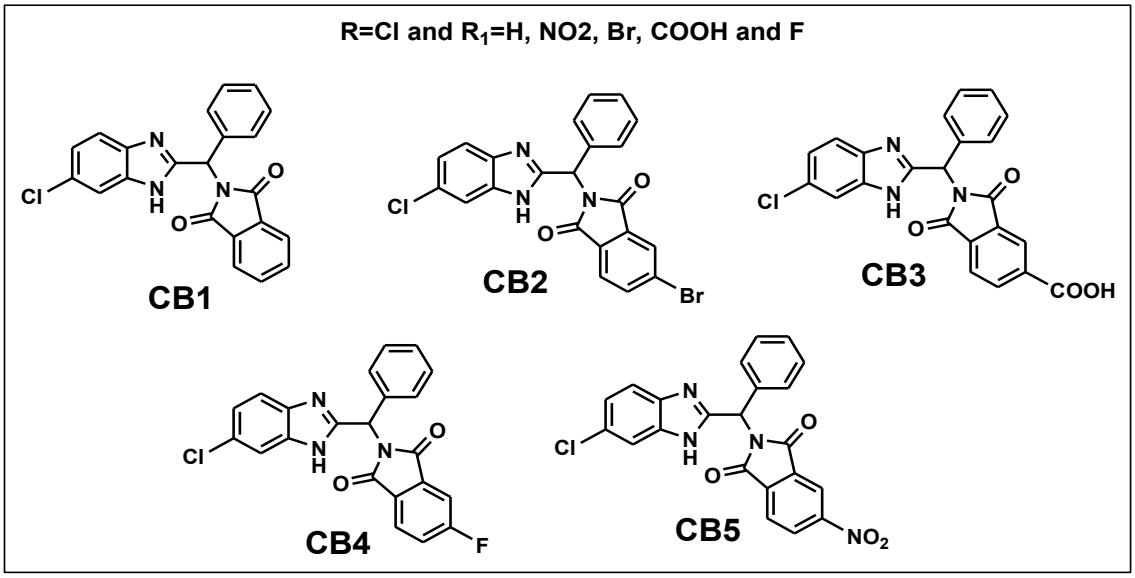
R=Cl and R1=H, NO2, Br, COOH and F
CB1
CB2
CB3
CB4
CB5

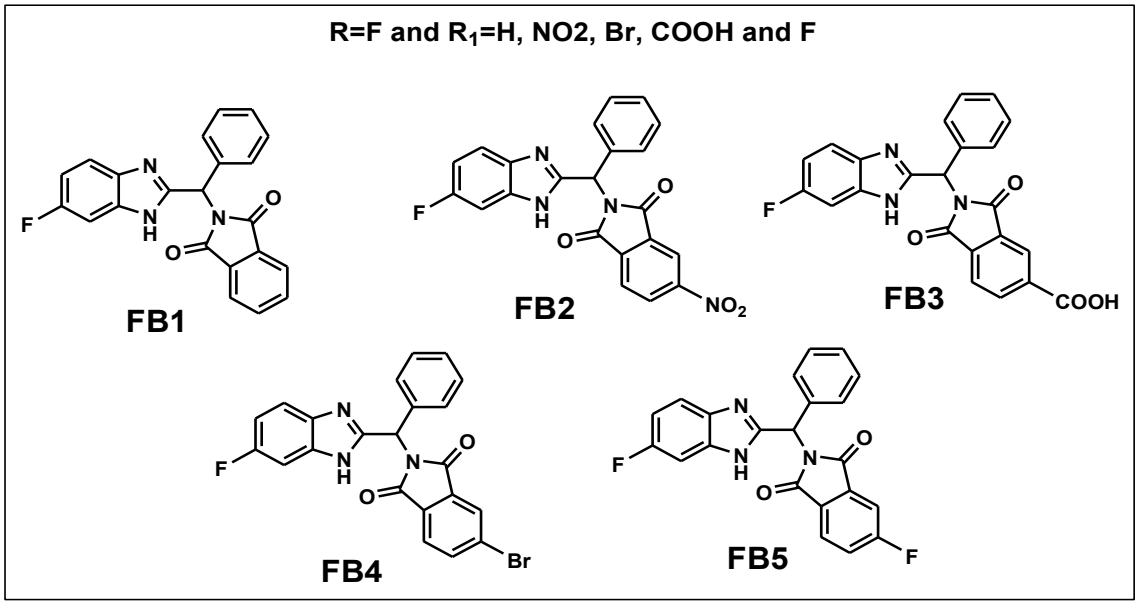
R=F and R1=H, NO2, Br, COOH and F
FB1
FB2
FB3
FB4
FB5

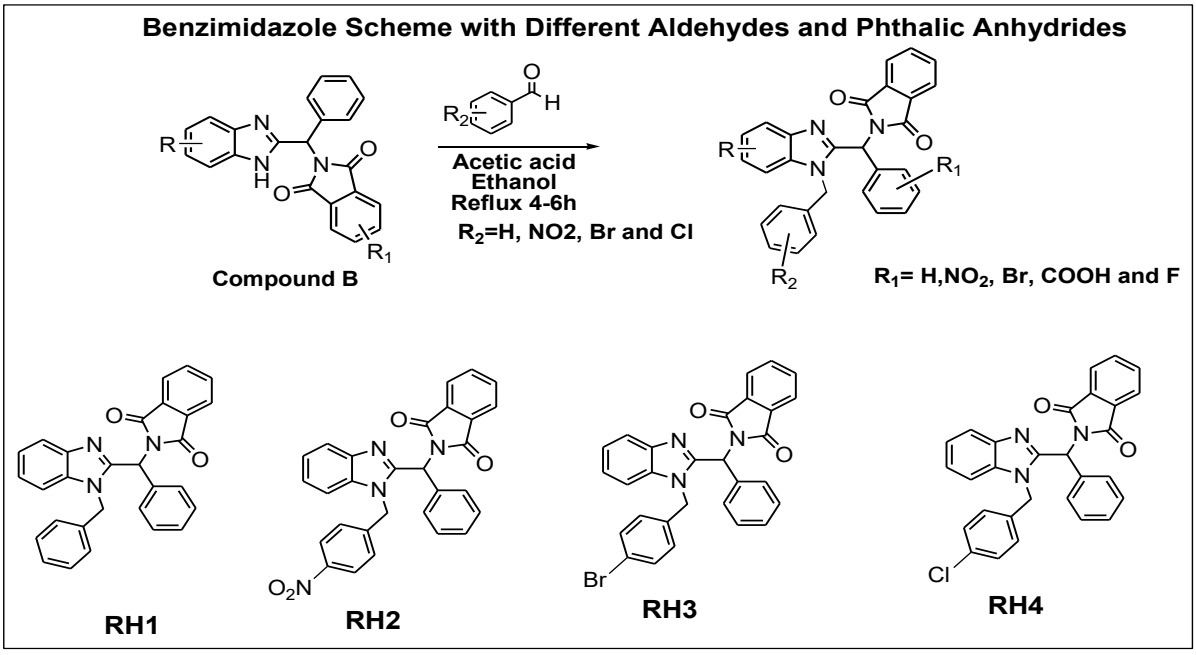
Benzimidazole Scheme with Different Aldehydes and Phthalic Anhydrides
Compound B
Acetic acid
Ethanol
Reflux 4-6h
R2=H, NO2, Br and Cl
R1= H,NO2, Br, COOH and F
RH1
RH2
RH3
RH4

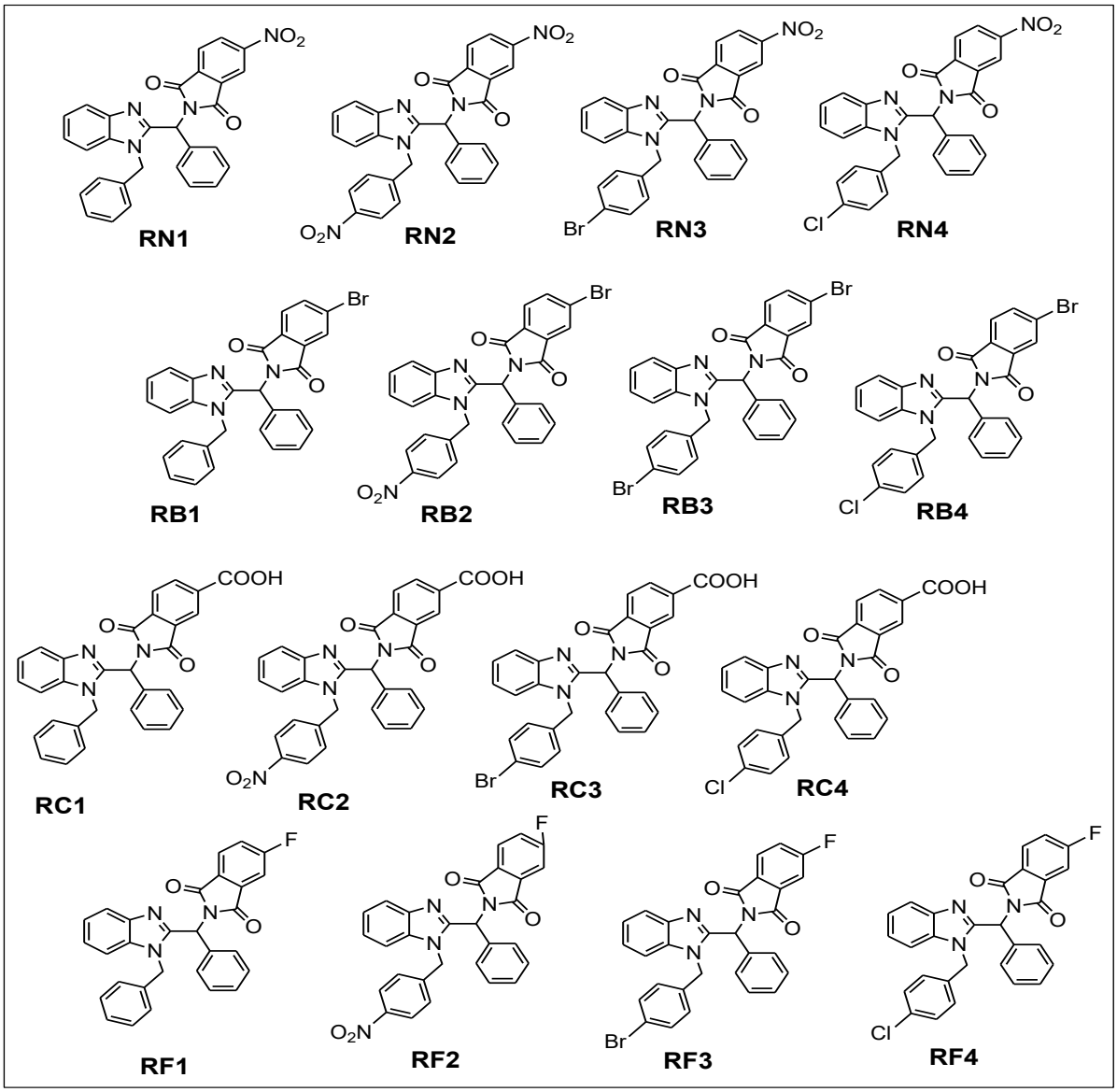

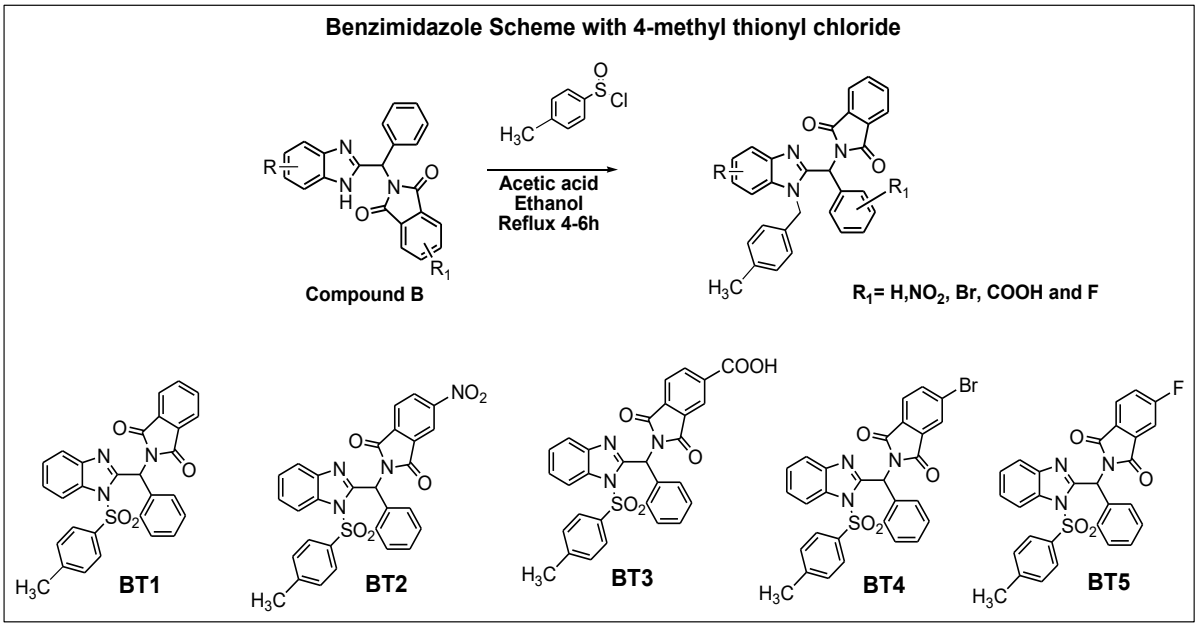

2.2.2 General Scheme for Isoxazole Based Derivatives

Compound 3 was prepared by coupling 1 with 3-hydroxybenzoic acid (2) using EDC.HCl as the activating agent in dry DMF at room temperature for 12 h, affording the intermediate 3 in 91% yield. Attempts to perform this coupling using HOBt/DICI resulted in a lower yield of 78%. Subsequently, various bromomethyl ketones were reacted with the solid-supported 3-hydroxybenzamide (3) in a 10% HMPA-DMF mixture, using DIPEA as the base under microwave irradiation, which furnished the polymer-bound intermediates 4 in excellent yields. Replacement of DIPEA with DBU led to a reduced yield of 67%. In the next step, the polymer-linked intermediates 4 were converted to the corresponding polymer-bound enamino ketones (5) via reaction with DMFDMA. Optimal conditions involved the use of dry DMF under microwave irradiation at 120 °C for 1 h, providing quantitative yields. The five-membered heterocyclization was carried out by treating intermediate 5 with hydroxylamine hydrochloride in a solvent mixture of DMF/i-PrOH (4:1) under microwave irradiation at 90 °C for 30 min, followed by cleavage from the resin. This sequence afforded the target isoxazole derivatives (6) in 50-70% yield [15-21].

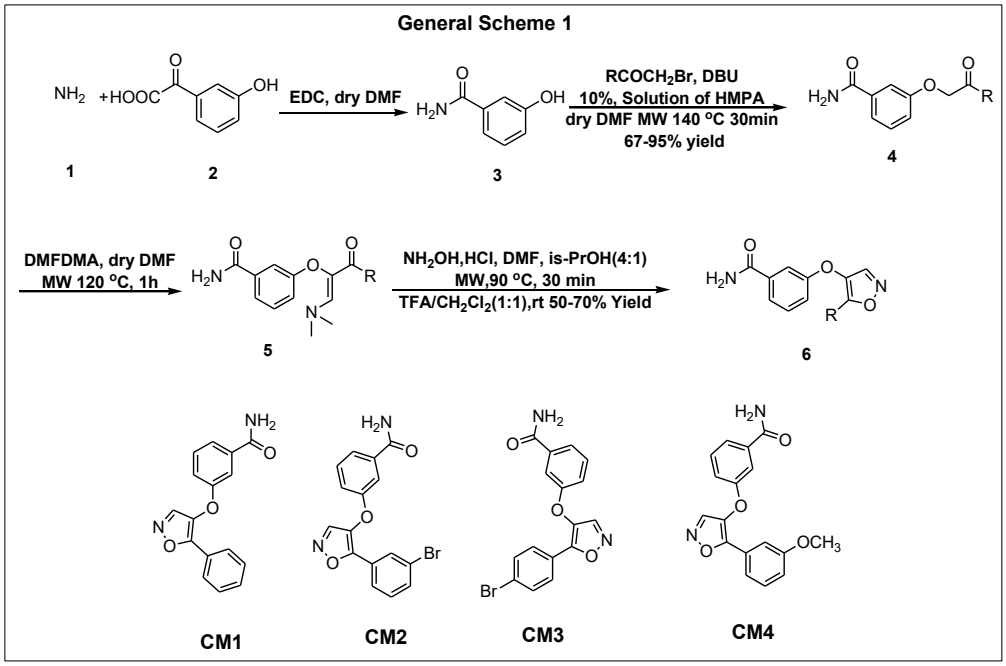

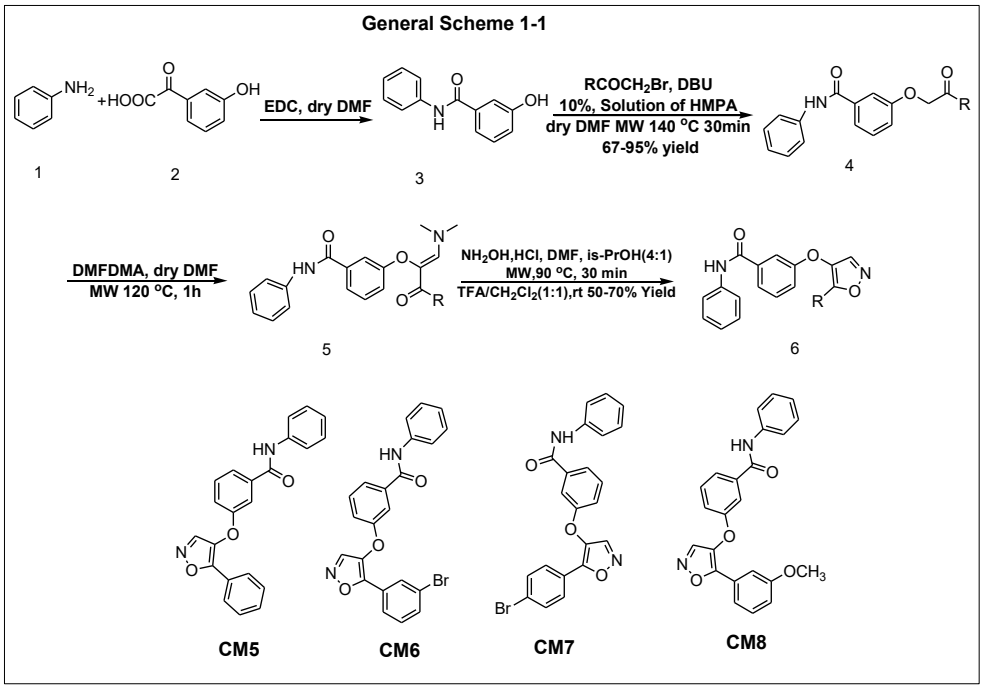

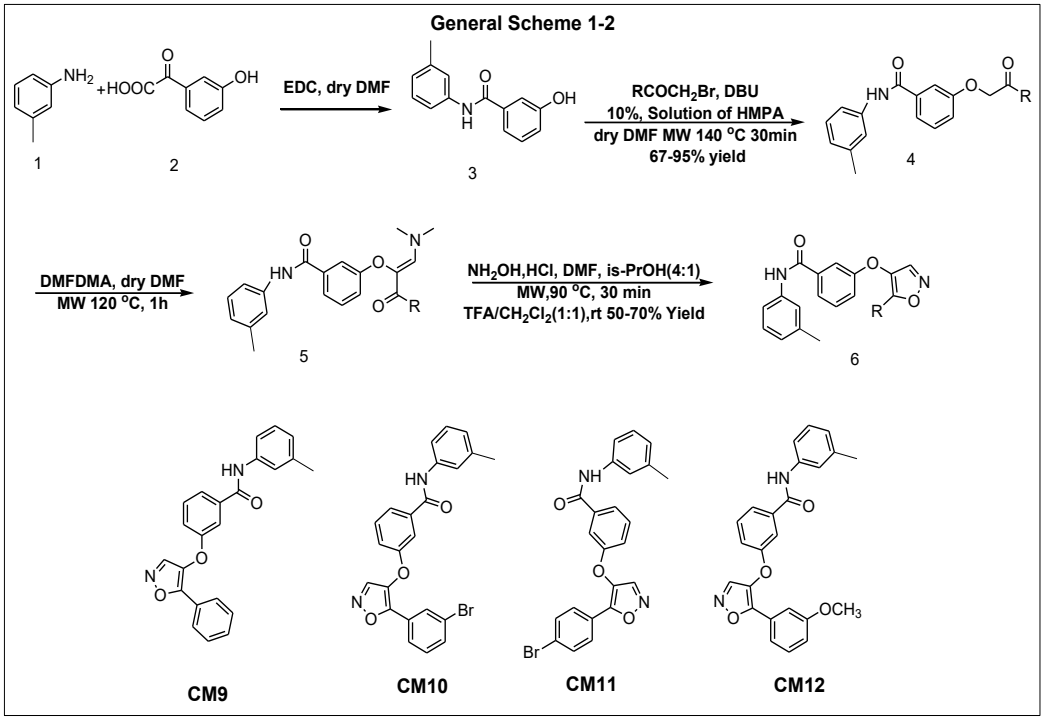
General Scheme 1-2
EDC, dry DMF
RCOCH2Br, DBU
10%, Solution of HMPA
dry DMF MW 140 °C 30min
67-95% yield
DMFDMA, dry DMF
MW 120 °C, 1h
NH2OH,HCl, DMF, is-PrOH(4:1)
MW,90 °C, 30 min
TFA/CH2Cl2(1:1),rt 50-70% Yield
1
2
3
4
5
6
CM9
CM10
CM11
CM12

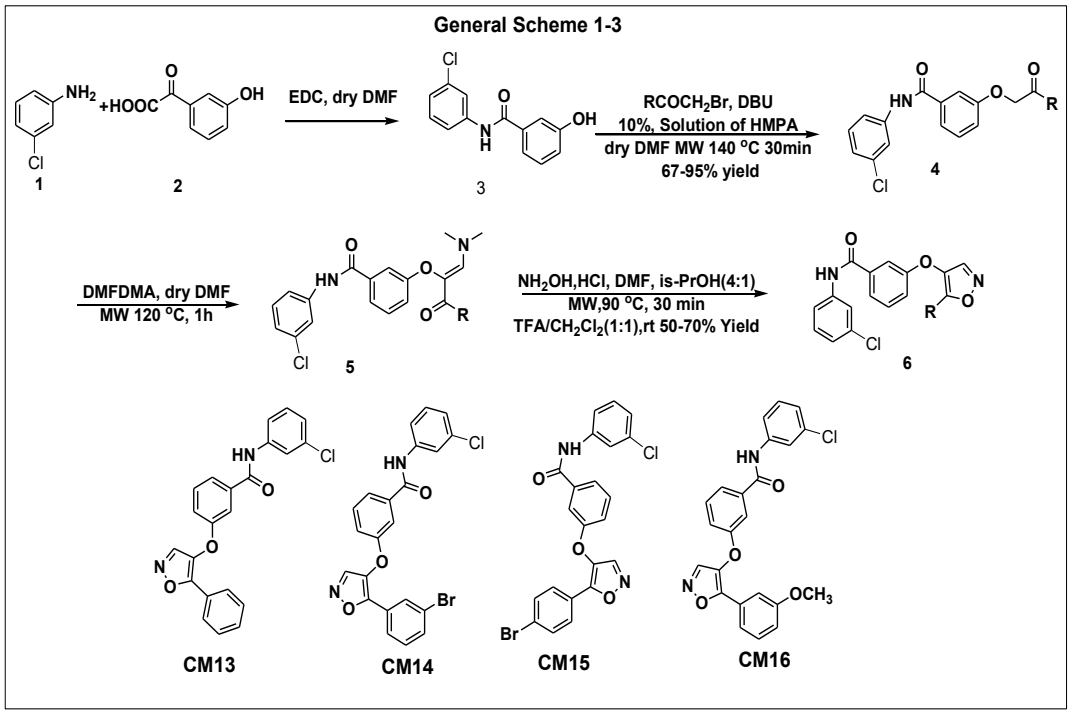
General Scheme 1-3
EDC, dry DMF
RCOCH2Br, DBU
10%, Solution of HMPA
dry DMF MW 140 °C 30min
67-95% yield
DMFDMA, dry DMF
MW 120 °C, 1h
NH2OH,HCl, DMF, is-PrOH(4:1)
MW,90 °C, 30 min
TFA/CH2Cl2(1:1),rt 50-70% Yield
1
2
3
4
5
6
CM13
CM14
CM15
CM16

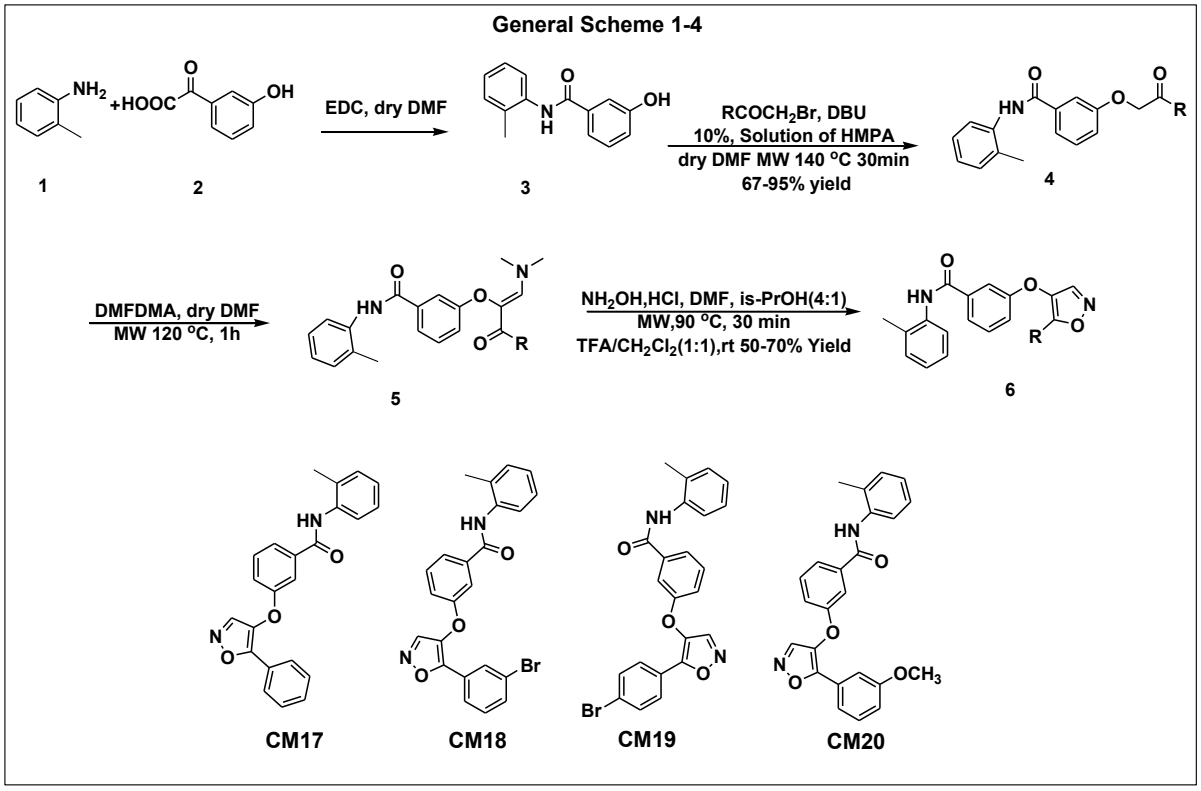
General Scheme 1-4
EDC, dry DMF
RCOCH2Br, DBU
10%, Solution of HMPA
dry DMF MW 140 °C 30min
67-95% yield
DMFDMA, dry DMF
MW 120 °C, 1h
NH2OH,HCl, DMF, is-PrOH(4:1)
MW,90 °C, 30 min
TFA/CH2Cl2(1:1),rt 50-70% Yield
1
2
3
4
5
6
CM17
CM18
CM19
CM20

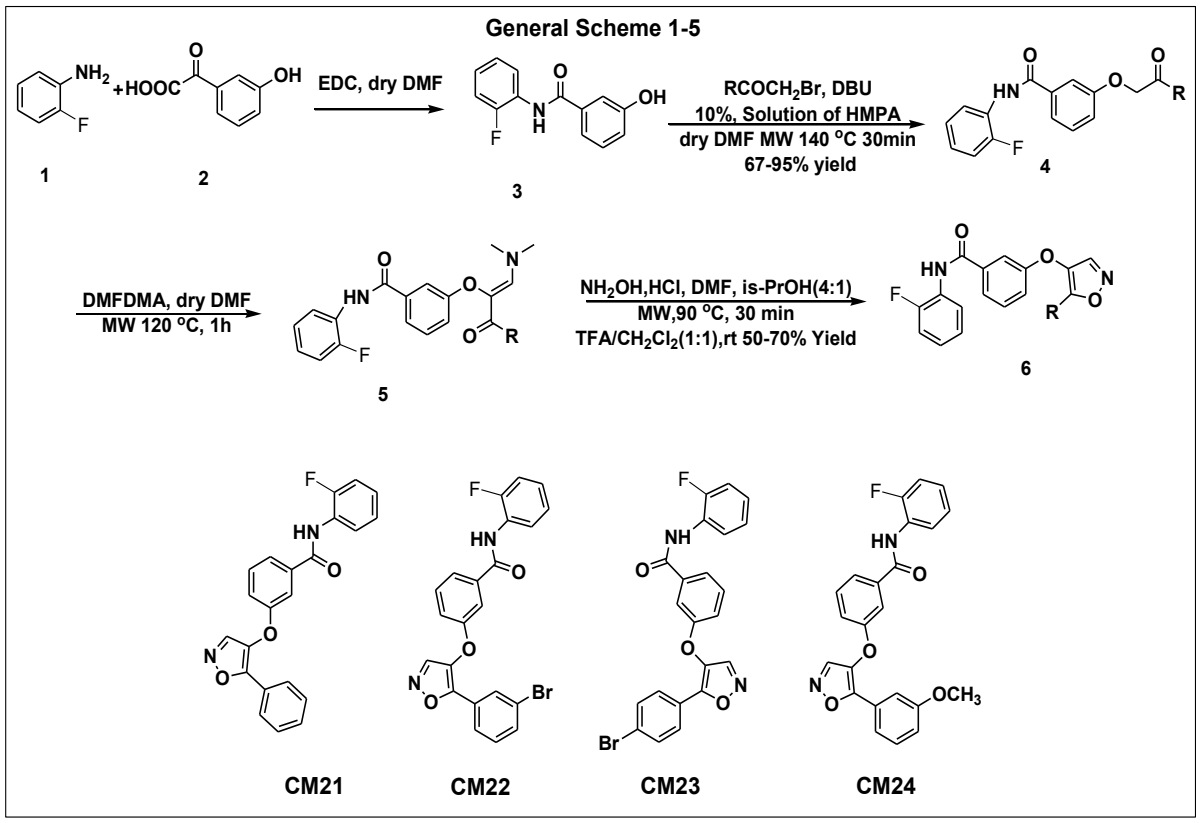
General Scheme 1-5
EDC, dry DMF
RCOCH2Br, DBU
10%, Solution of HMPA
dry DMF MW 140 °C 30min
67-95% yield
DMFDMA, dry DMF
MW 120 °C, 1h
NH2OH,HCl, DMF, is-PrOH(4:1)
MW,90 °C, 30 min
TFA/CH2Cl2(1:1),rt 50-70% Yield
1
2
3
4
5
6
CM21
CM22
CM23
CM24

General Scheme 2

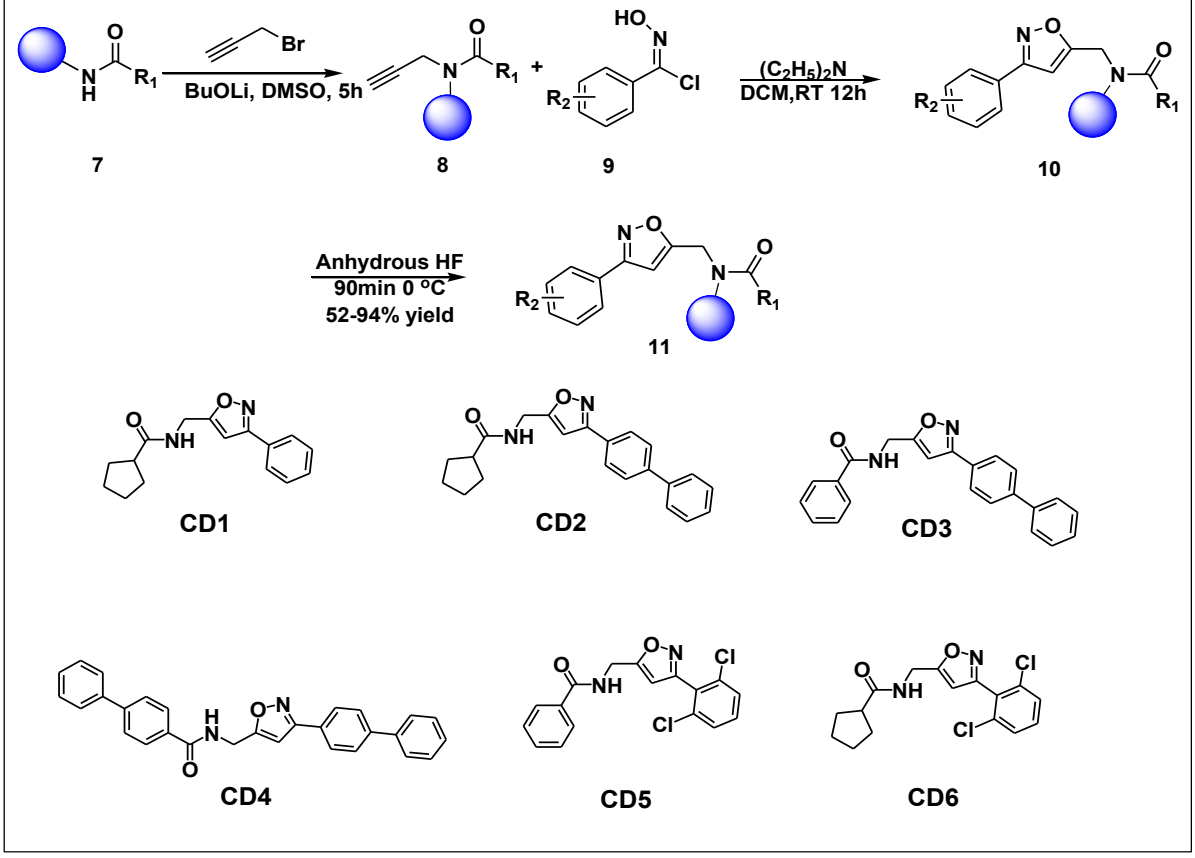

General Scheme 2-1

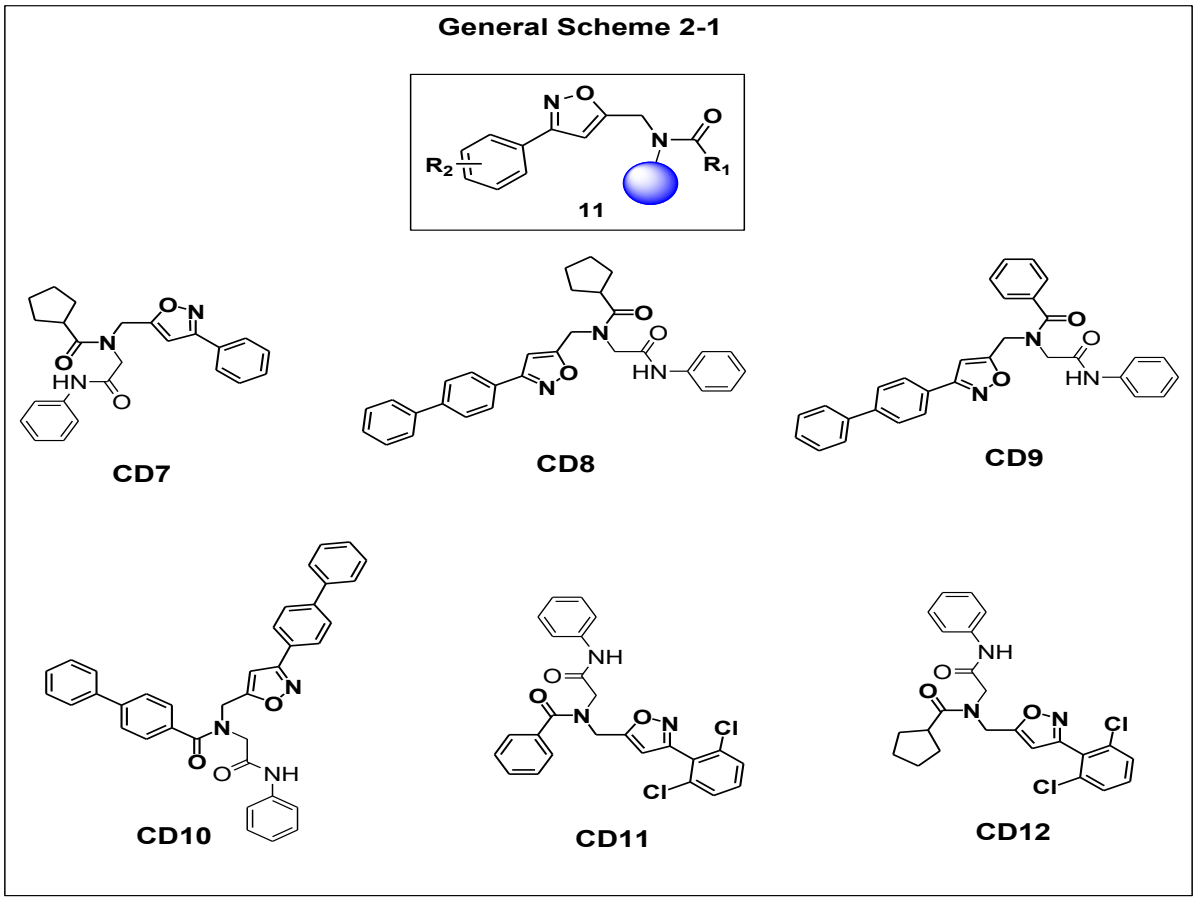

General Scheme 2-2

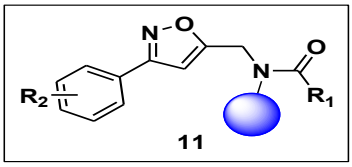

11

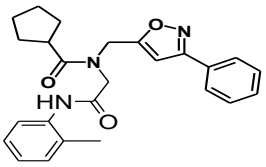

CD13

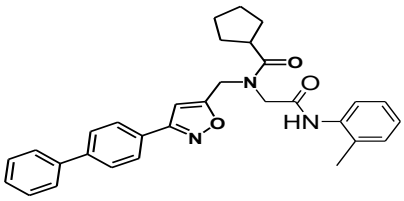

CD14

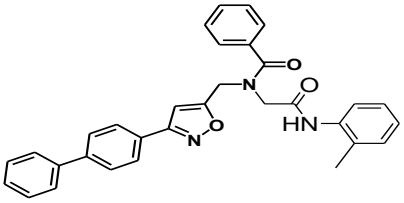

CD15

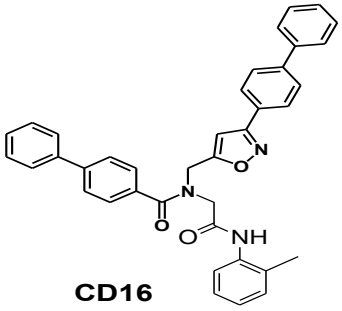

CD16

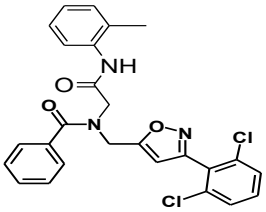

CD17

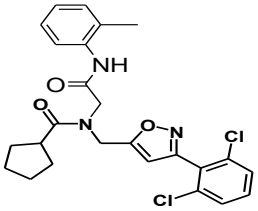

CD18

General Scheme 2-3

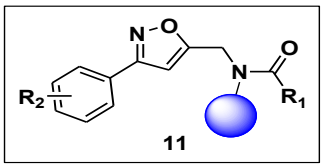

11

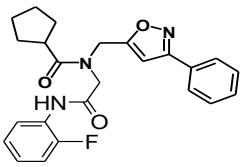

CD19

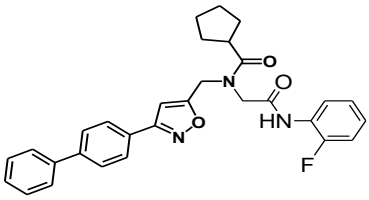

CD20

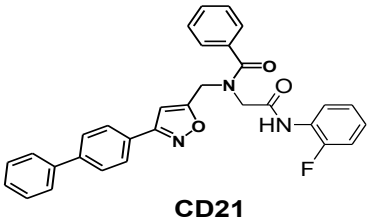

CD21

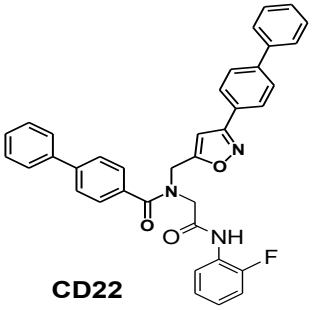

CD22

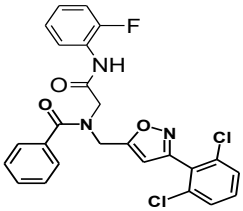

CD23

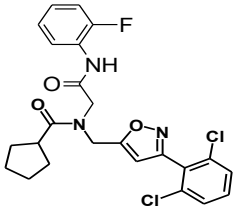

CD24

2.3 Molecular Docking Analysis

Docking simulations were carried out against crystal structure of complex formed between russell's viper phospholipase A2 and an anti-inflammatory agent oxyphenbutazone using standardized computational protocols. The target protein (PDB ID: 1Q7A) was obtained from the Protein Data Bank and selected for its high resolution (1.6 Å) and established relevance to anti-inflammatory mechanisms. During protein preparation, crystallographic water molecules, ions, and the co-crystallized ligand were retained or removed based on their structural and functional significance. All designed derivatives were docked into the active site and key molecular interactions were analysed to evaluate their binding profiles and pharmacological potential.

2.4 Characterization of Synthesized Derivatives

2.4.1 IR Spectroscopy

IR(KBr) spectra υ,cm-1 were recorded using Thermo Scientific™ Nicolet™ iS™10 FT-IR Spectrometer in Pioneer company for pharmaceutical industry-Sulaimani-Kurdistan-Iraq.

2.4.2 NMR Spectroscopy

^{13}C-NMR spectra were recorded on Bruker FT–NMR spectrophotometer 400, using deuterated dimethyl sulfoxide (DMSO-$_{d6}$) and deuterated chloroform ($CDCl_3$) as internal standards. Chemical shifts were expressed in δ ppm.

2.4.3 Mass Spectroscopy

MS was run, using Agilent Technology (HP), GC/MS model 5973 network mass selective detector. The values were expressed as m/z.

2.5 In-vivo Evaluation of Anti-Inflammatory Activity

2.5.1 Experimental Animals

Healthy 48 albino rats were procured and maintained in the animal house of R.V. Northland Institute, Dadri, under the reg. no: RVN1/1AEC/24-25/15. Rats were kept in sterilized polypropylene cages lined with paddy husk. The animals were maintained under a regulated 12-hour light: 12-hour dark scheduled at room temperature. Ethical clearance was obtained from the Institute animal Ethics Committee for handling the experimental animals.

2.5.2 Dose Preparation of Synthesized Compound

Based on the *in-silico* study results, the six synthesized compounds (MB3, FB5, BT4, CD4, CD16, and CD22) represented favourable binding profiles were selected for in-vivo evaluation. The six synthesized compound were evaluated for their anti-inflammatory activity based on *in-silico* toxicity guided dose selection. The acute toxicity (LD_{50}) of each compound was first predicted using computational toxicity assessment tools. To ensure safety and avoid the potential toxic manifestations during biological evaluation, the in-vivo test dose for each compound was fixed at one-tenth (1/10th) of its predicted LD_{50} dose.

Following purification, each compound was accurately weighed and dissolved in sterile normal saline to prepare the required dose concentration. Healthy 48 albino rats were divided into eight groups in which the control group (normal saline), a standard group (diclofenac sodium, 10 mg/kg), and six test groups of each synthesized compound. The anti-inflammatory activity was assessed using the carrageenan-induced paw edema model, where animals received the test dose orally one hour prior to carrageenan injection (0.1 ml of 1% solution) into the hind paw. The paw volume was measured at different interval of time after injection using a digital plethysmometer and the percentage inhibition of edema was calculated relative to control [22].

3. RESULT & DISCUSSION

3.1 Synthesis

Based on *in-silico* study result, the six compounds (code; MB3, FB5, BT4, CD4, CD16, and CD22) were successfully synthesized with yields ranging from 60% to 85%. The reactions proceeded smoothly, and the final compounds were obtained as crystalline solids.

3.2 Molecular Docking Analysis

The molecular docking studies were conducted using the Autodock Vina which represented the compound code (MB3, FB5, BT4, CD4, CD16, and CD22) exhibited most favourable binding score and exhibited varying binding affinities towards the selected inflammatory target. The binding affinity score indicated strong and stable interactions through multiple hydrogen bonds and hydrophobic contacts within the active site. The docking result of all designed compound were presented in table 1 and 2.

Table 1. Outcomes of Molecular Docking Studies for Benzimidazole Based Derivatives

Compound Code	Docking Score (kcal/mol)	Compound Code	Docking Score (kcal/mol)	Compound Code	Docking Score (kcal/mol)
PB1	-9.3	FB1	-9.7	RB3	-6.8
PB2	-9.3	FB2	-9.7	RB4	-8.0
PB3	-9.1	FB3	-9.5	RC1	-7.9
PB4	-9.5	FB4	-9.2	RC2	-9.1
PB5	-9.3	**FB5**	**-10.9**	RC3	-6.6
MB1	-9.5	RH1	-6.7	RC4	-7.6
MB2	-9.6	RH2	-6.8	RF1	-9.2
MB3	**-10.3**	RH3	-9.8	RF2	-9.8
MB4	-9.6	RH4	-8.8	RF3	-7.9
MB5	-8.8	RN1	-8.5	RF4	-8.3
CB1	-6.3	RN2	-8.4	BT1	-9.3

CB2	-9.6	RN3	-8.6	BT2	-6.2
CB3	-8.2	RN4	-7.9	BT3	-7.1
CB4	-9.5	RB1	-7.5	**BT4**	**-9.9**
CB5	-8.5	RB2	-8.7	BT5	-6.1
Reference Drug (Diclofenac): -7.2 (kcal/mol)					

Table 2. Outcomes of Molecular Docking Studies for Isoxazole Based Derivatives

Compound Code	**Docking Score (kcal/mol)**	**Compound Code**	**Docking Score (kcal/mol)**
CM1	-8.2	CD1	-8.1
CM2	-8.4	CD2	-9.5
CM3	-8.3	CD3	-9.7
CM4	-8.1	**CD4**	**-10.2**
CM5	-9.6	CD5	-8.5
CM6	-9.4	CD6	-7.9
CM7	-9.3	CD7	-8.6
CM8	-9.3	CD8	-9.2
CM9	-9.8	CD9	-9.7
CM10	-9.6	CD10	-9.7
CM11	-9.5	CD11	-8.8
CM12	-9.3	CD12	-8.7
CM13	-9.5	CD13	-8.6
CM14	-9.5	CD14	-9.1
CM15	-9.2	CD15	-7.3
CM16	-9.2	**CD16**	**-10.1**
CM17	-9.6	CD17	-9.1
CM18	-9.7	CD18	-9.1
CM19	-9.4	CD19	-8.9
CM20	-9.4	CD20	-7.4
CM21	-9.8	CD21	-9.8
CM22	-9.7	**CD22**	**-10.6**
CM23	-9.8	CD23	-9.0
CM24	-9.6	CD24	-8.9
Reference Drug (Diclofenac): -7.3 (kcal/mol)			

Among all screened molecules, the six compound (code; MB3, FB5, BT4, CD4, CD16, and CD22) exhibited the most favourable binding affinities and interaction patterns. Their detailed interaction profiles with the target protein are presented in Figure 1 to 6.

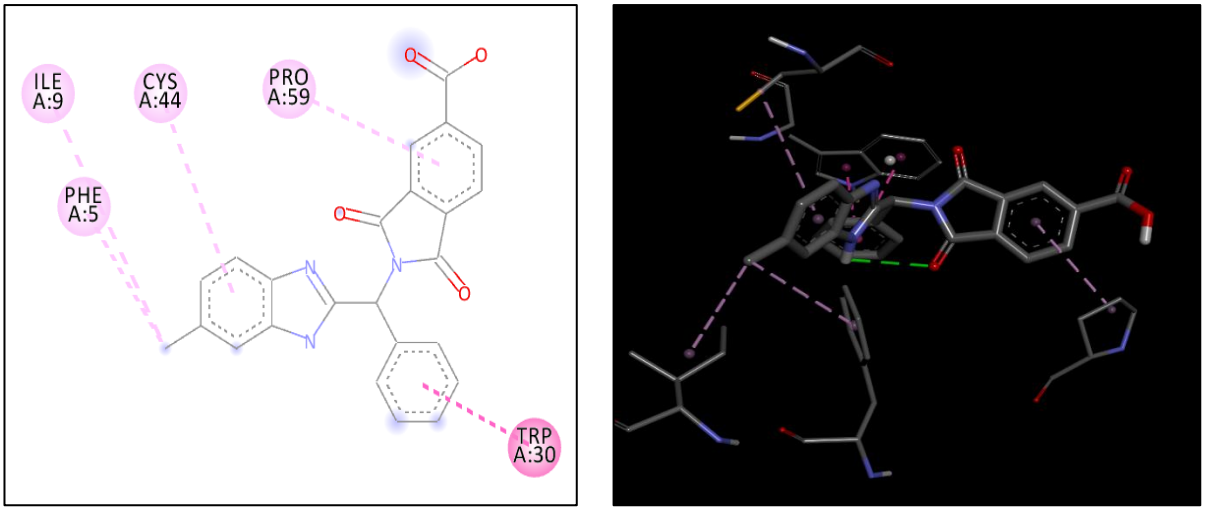

Figure 1. Docking Result and Interaction of Compound Code MB3

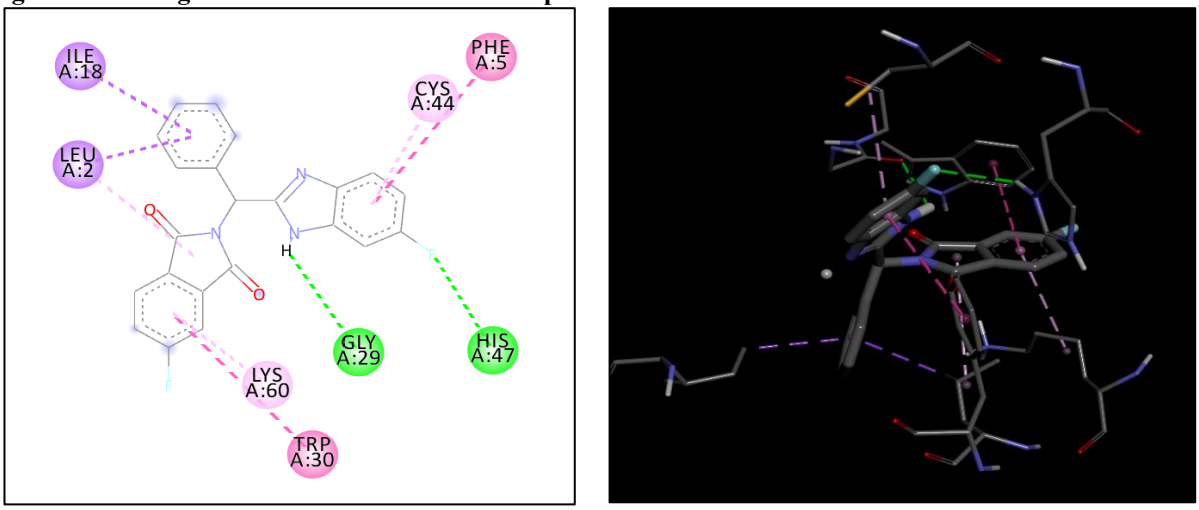

Figure 2. Docking Result and Interaction of Compound Code FB5

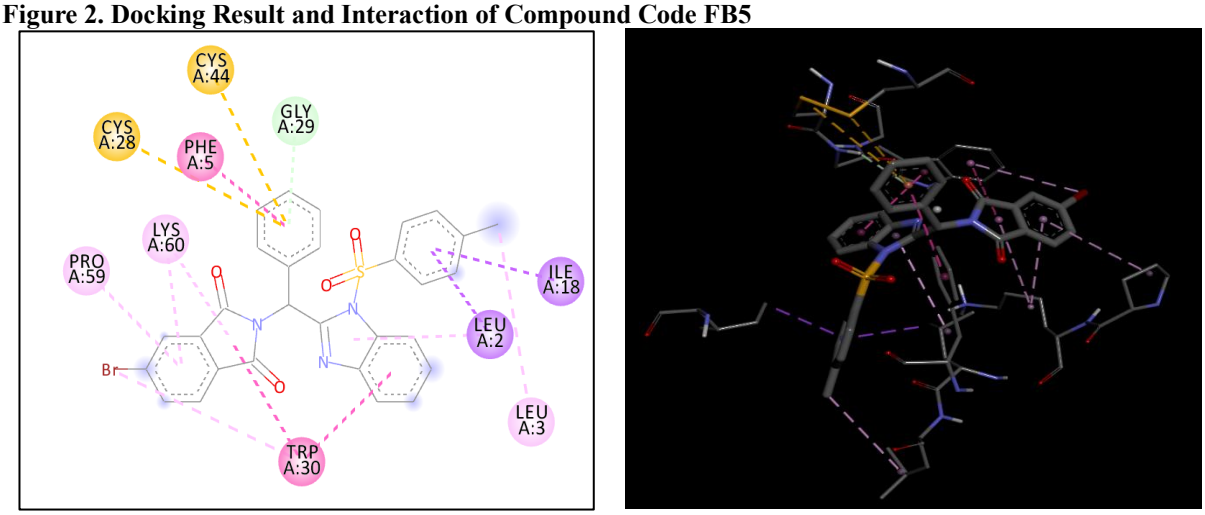

Figure 3. Docking Result and Interaction of Compound Code BT4

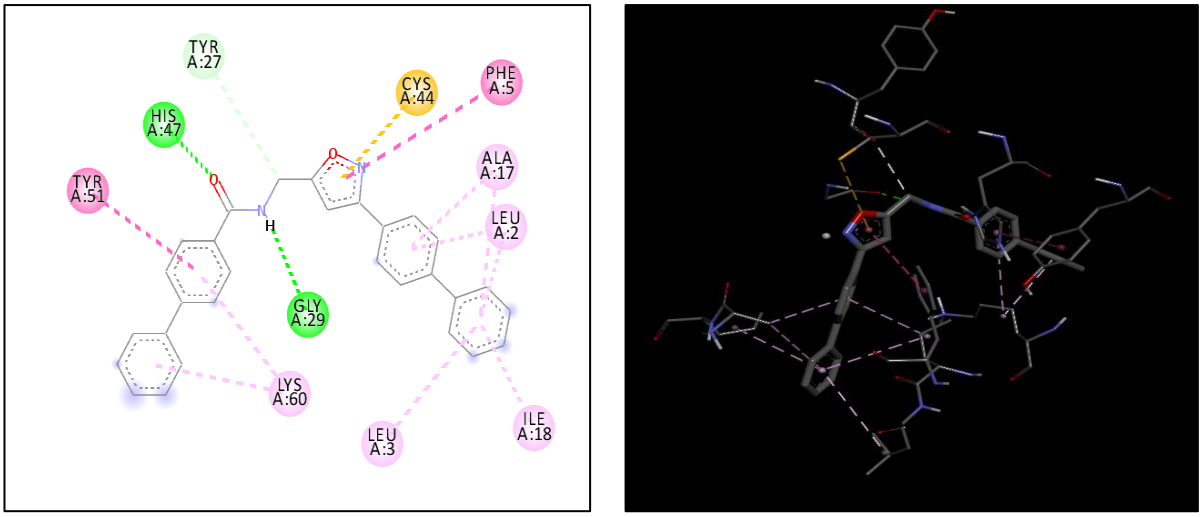

Figure 4. Docking Result and Interaction of Compound Code CD4

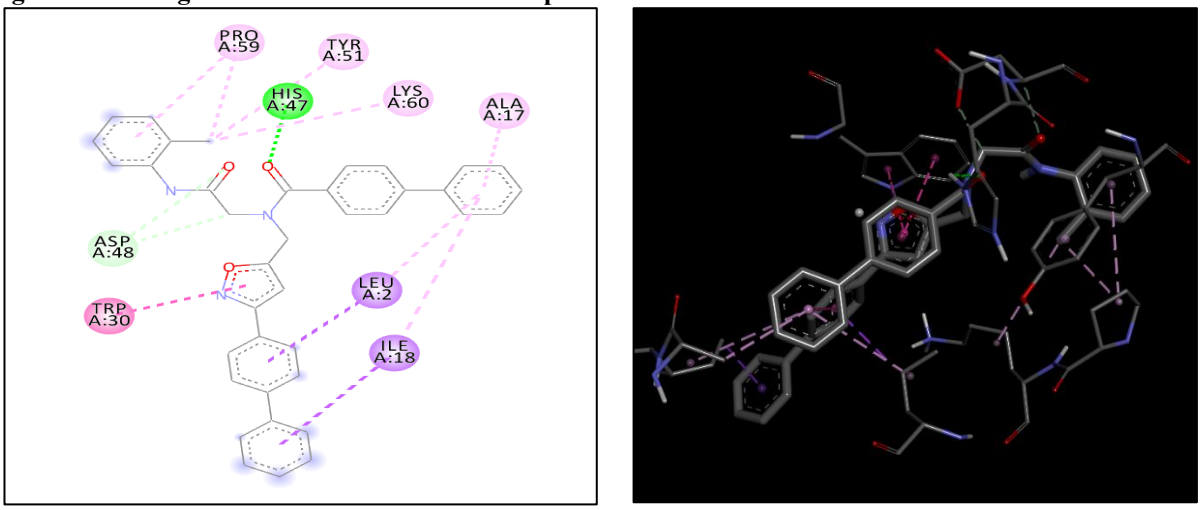

Figure 5. Docking Result and Interaction of Compound Code CD16

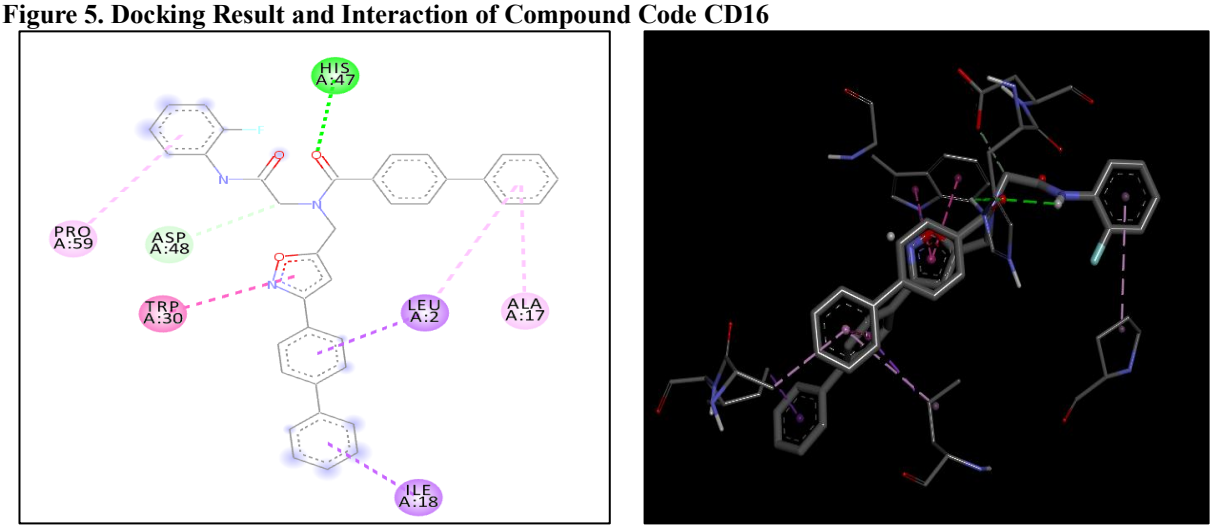

Figure 6. Docking Result and Interaction of Compound Code CD22

3.3 Spectral Characterization

The synthesized derivatives such as MB3, FB5, BT4, CD4, CD16, and CD22 were characterized using IR, ^{1}H NMR, ^{13}C NMR, and mass spectrometry, all of which confirmed structures consistent with the expected molecular frameworks.

3.3.1 Spectral Characterization of Compound Code MB3

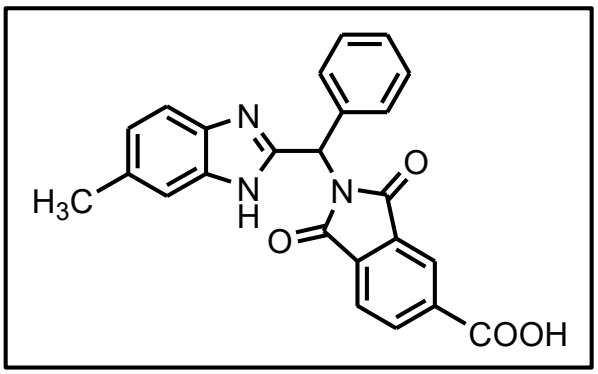

IR (KBr, cm^{-1}) 1687.79 (C=O), 3228.01 (N-H $_{str}$), 1599.06 (C=N), 3278.23 (OH $_{acid}$).

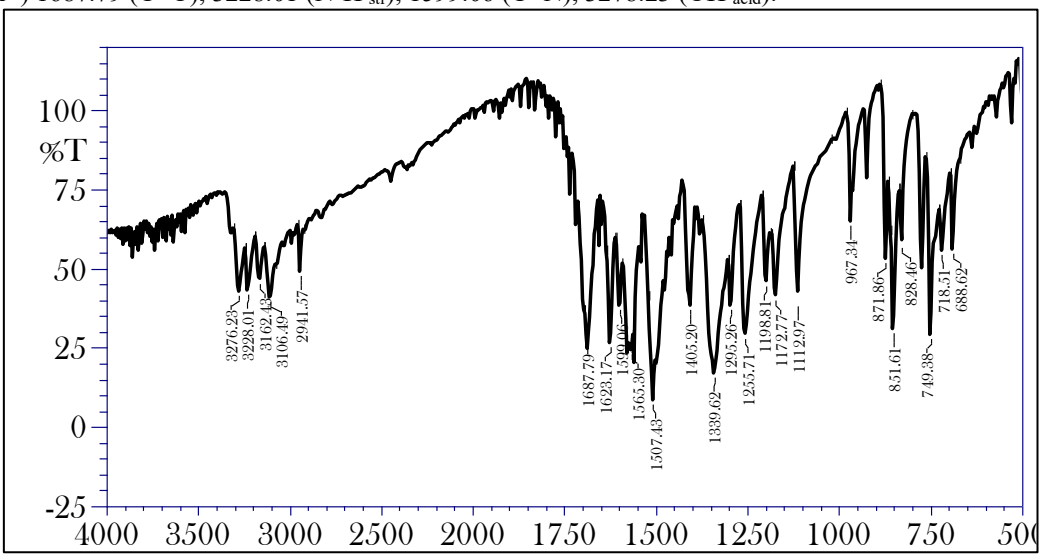

Figure 7. IR Spectra of Compound Code MB3

^{1}H NMR (500 MHz, Chloroform-*d*) δ 8.28 (dd, *J* = 8.1, 1.5 Hz, 1H), 8.23 (d, *J* = 1.5 Hz, 1H), 7.98 (d, *J* = 8.0 Hz, 1H), 7.42 – 7.30 (m, 6H), 7.33 – 7.21 (m, 2H), 7.10 (d, *J* = 0.9 Hz, 1H).

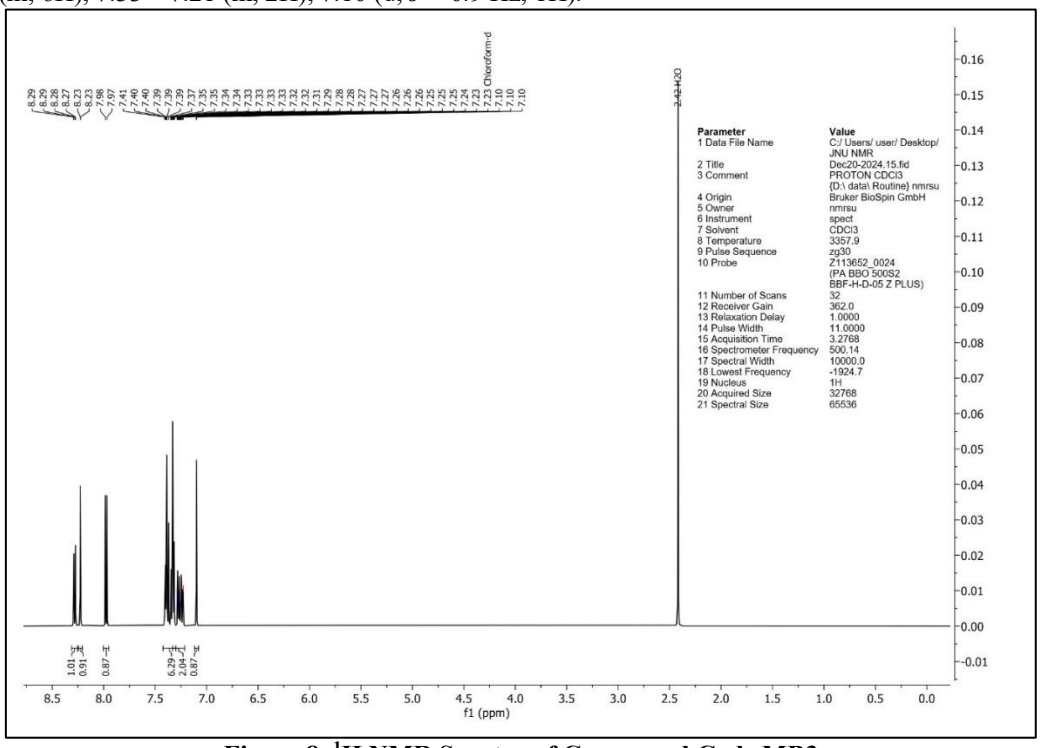

Figure 8. ^{1}H NMR Spectra of Compound Code MB3

^{13}C NMR (125 MHz, Chloroform-d) δ 169.69, 169.45, 168.63, 151.20, 136.88, 135.92, 135.86, 135.69, 134.35, 133.63, 131.73, 131.58, 128.41, 128.39, 128.24, 126.97, 123.79, 123.37, 114.61, 113.69, 58.03, 21.36.

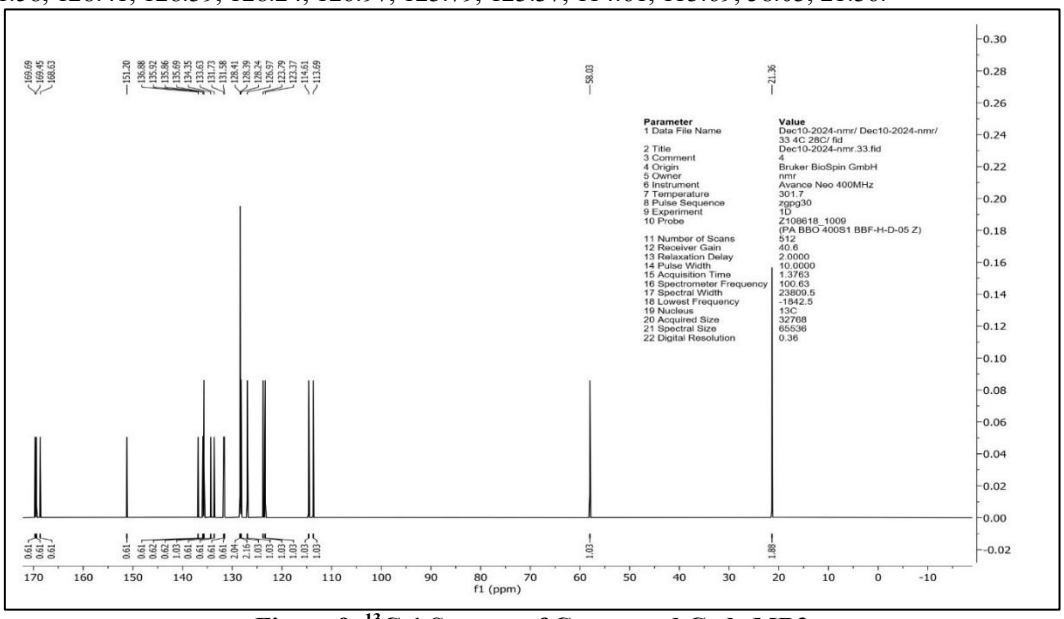

Figure 9. ^{13}C-1 Spectra of Compound Code MB3

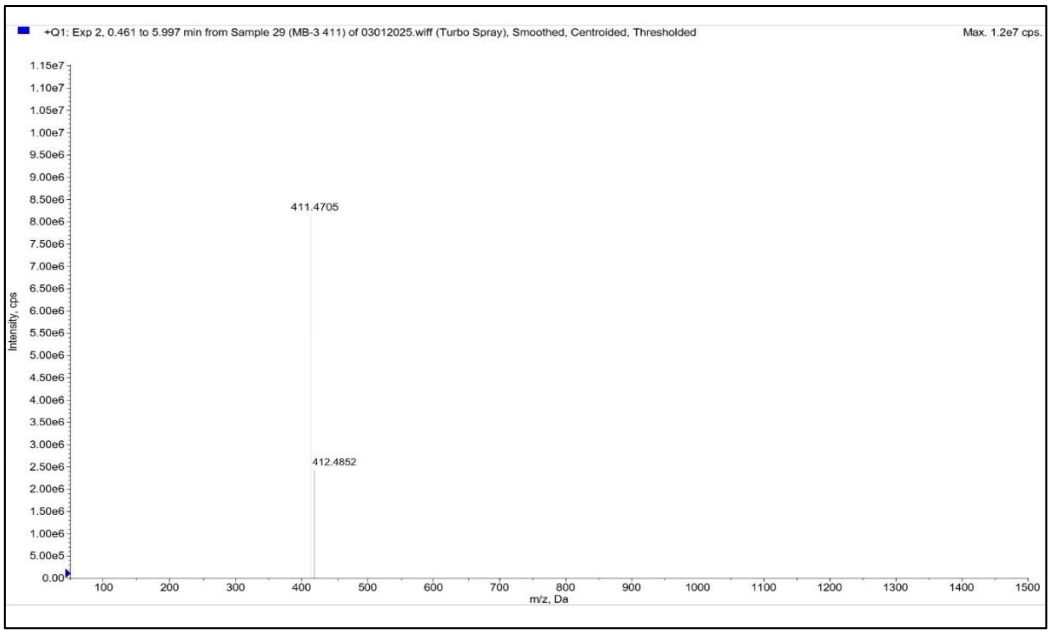

Figure 10. Mass Spectra of Compound Code MB3

3.3.2 Spectral Characterization of Compound Code FB5

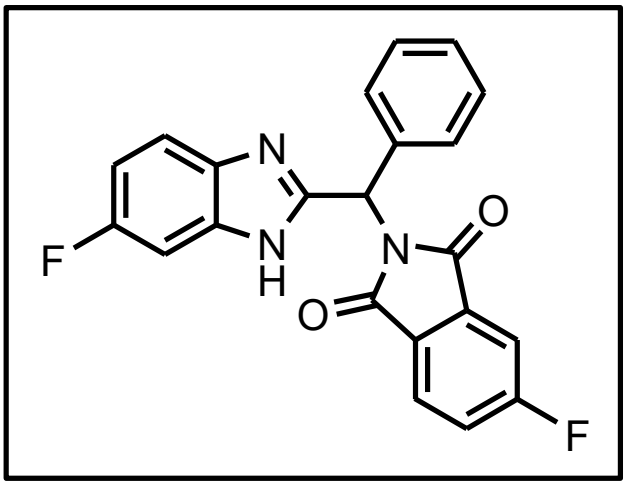

IR (KBr, cm^{-1}) 1661.75 (C=O), 3447.91 (N-H_{str}), 1457.28 (C=N), 1266.32 (C-F).

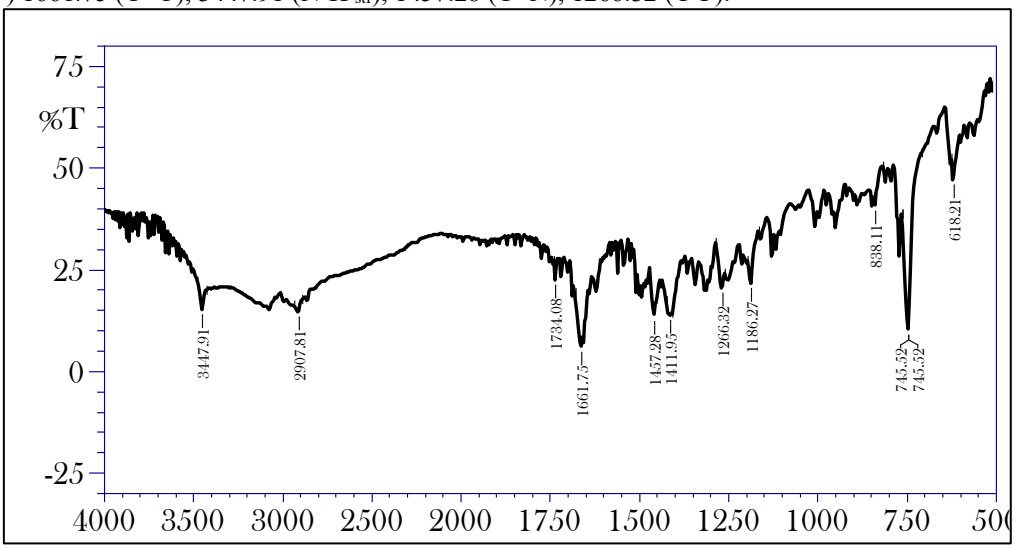

Figure 11. IR Spectra of Compound Code FB5

^{1}H NMR (500 MHz, Chloroform-*d*) δ 7.85 – 7.76 (m, 1H), 7.72 – 7.63 (m, 1H), 7.44 – 7.16 (m, 3H), 7.09 (d, *J* = 0.9 Hz, 1H)

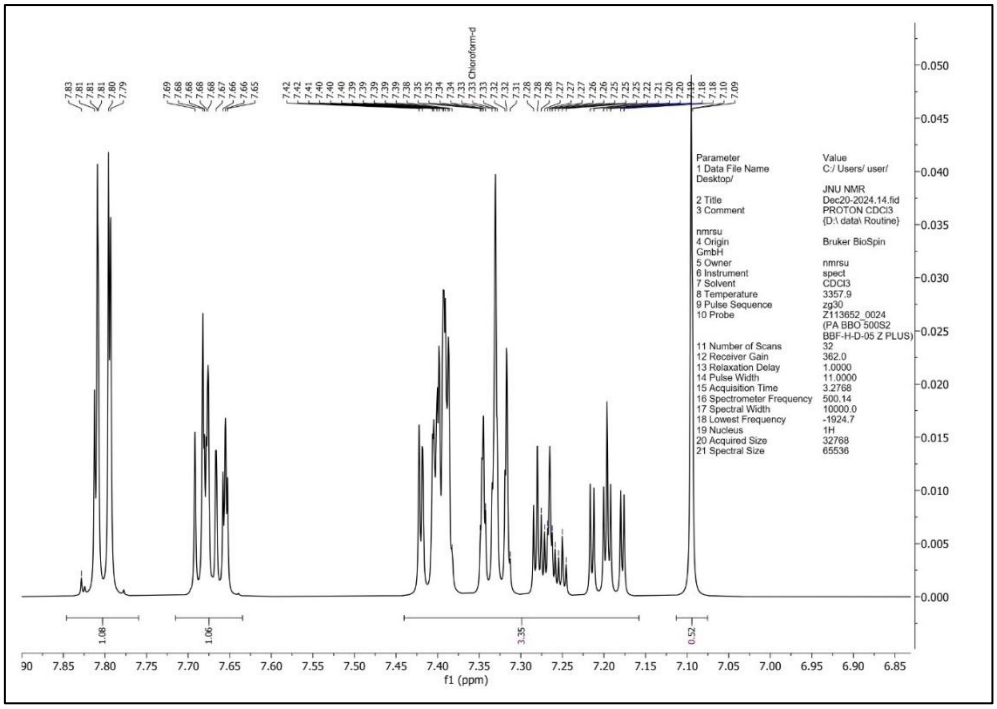

Figure 12. ^{1}H NMR Spectra of Compound Code FB5

^{13}C NMR (125 MHz, Chloroform-d) δ 169.69, 169.18, 169.14, 166.55, 164.58, 160.51, 158.54, 151.65, 138.30, 138.21, 136.88, 135.33, 135.30, 131.76, 131.69, 128.41, 128.39, 128.26, 128.24, 125.51, 125.44, 122.25, 122.07, 118.45, 118.38, 111.98, 111.79, 111.13, 110.95, 101.39, 101.19, 58.04.

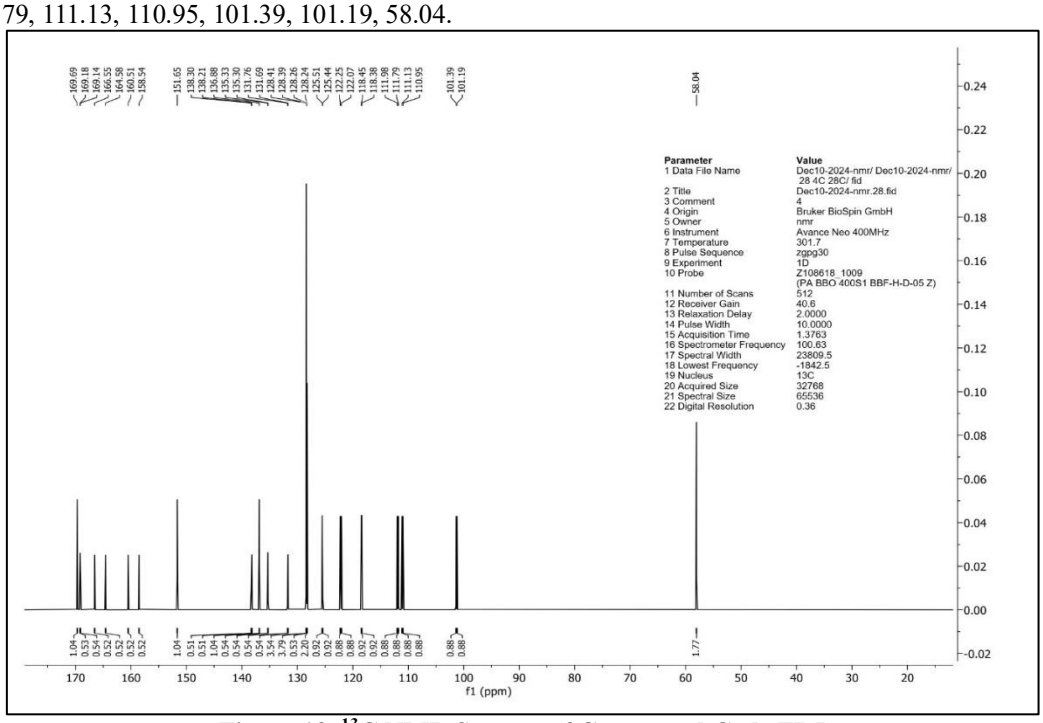

Figure 13. ^{13}C NMR Spectra of Compound Code FB5

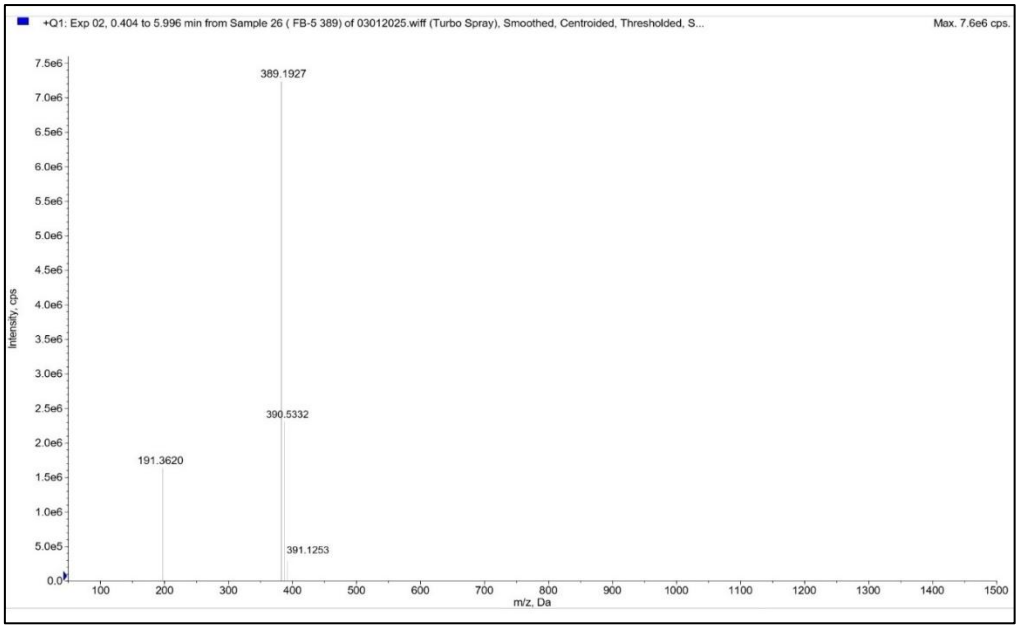

Figure 14. Mass Spectra of Compound Code FB5

3.3.3 Spectral Characterization of Compound Code BT4

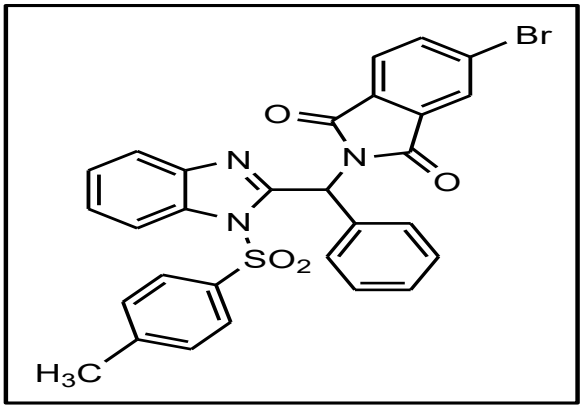

IR (KBr, cm^{-1}) 1684.89 (C=O), 3038.98 (N-H $_{str}$), 1599.06 (C=N), 2363.87 (C-Br), 1184.34 (C-SO_2).

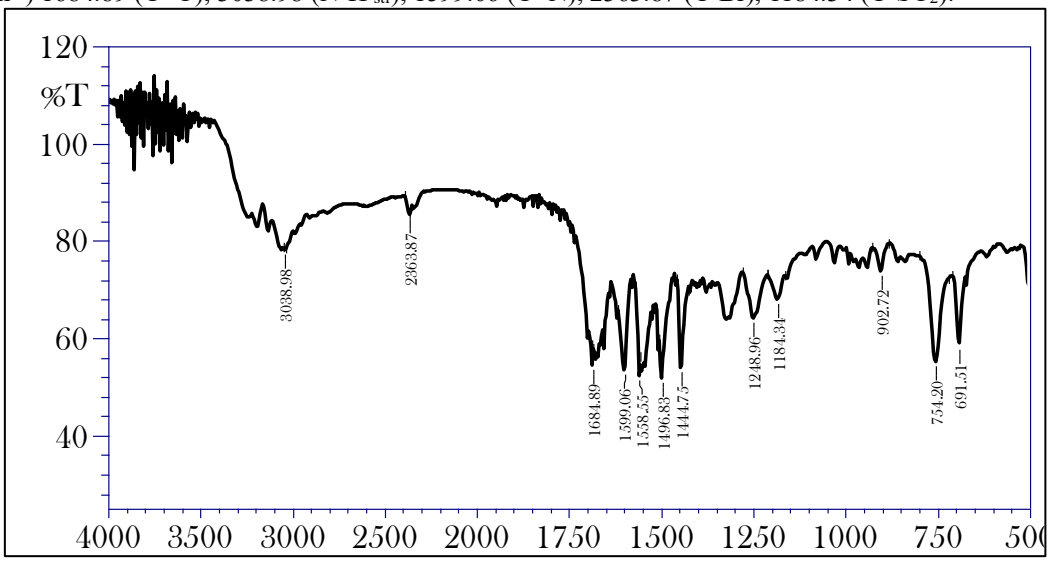

Figure 15. IR Spectra of Compound Code BT4

^{1}H NMR (500 MHz, Chloroform-*d*) δ 8.11 (d, *J* = 2.6 Hz, 1H), 8.04 – 7.98 (m, 2H), 7.96 (dd, *J* = 7.4, 1.5 Hz, 1H), 7.89 (dd, *J* = 7.9, 2.6 Hz, 1H), 7.81 (dd, *J* = 6.7, 1.5 Hz, 1H), 7.74 – 7.68 (m, 2H), 7.53 (td, *J* = 7.2, 1.3 Hz, 1H), 7.44 (td, *J* = 6.9, 1.4 Hz, 1H), 7.40 (dtd, *J* = 6.1, 2.5, 1.4 Hz, 2H), 7.36 – 7.23 (m, 2H), 7.22 – 7.16 (m, 2H).

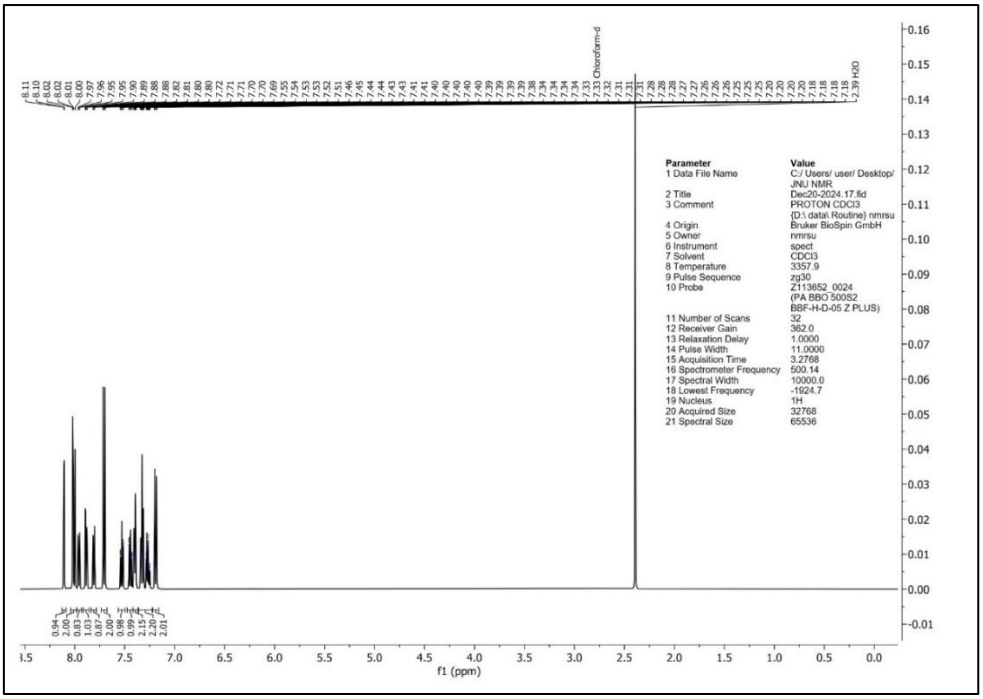

Figure 16. ^{1}H NMR Spectra of Compound Code BT4

^{13}C NMR (125 MHz, Chloroform-d) δ 168.45, 168.35, 154.28, 142.74, 141.42, 137.67, 136.85, 136.78, 134.96, 132.34, 130.17, 129.63, 128.68, 128.41, 128.25, 126.99, 126.95, 126.08, 125.79, 124.46, 123.91, 121.44, 114.87, 57.00, 21.56.

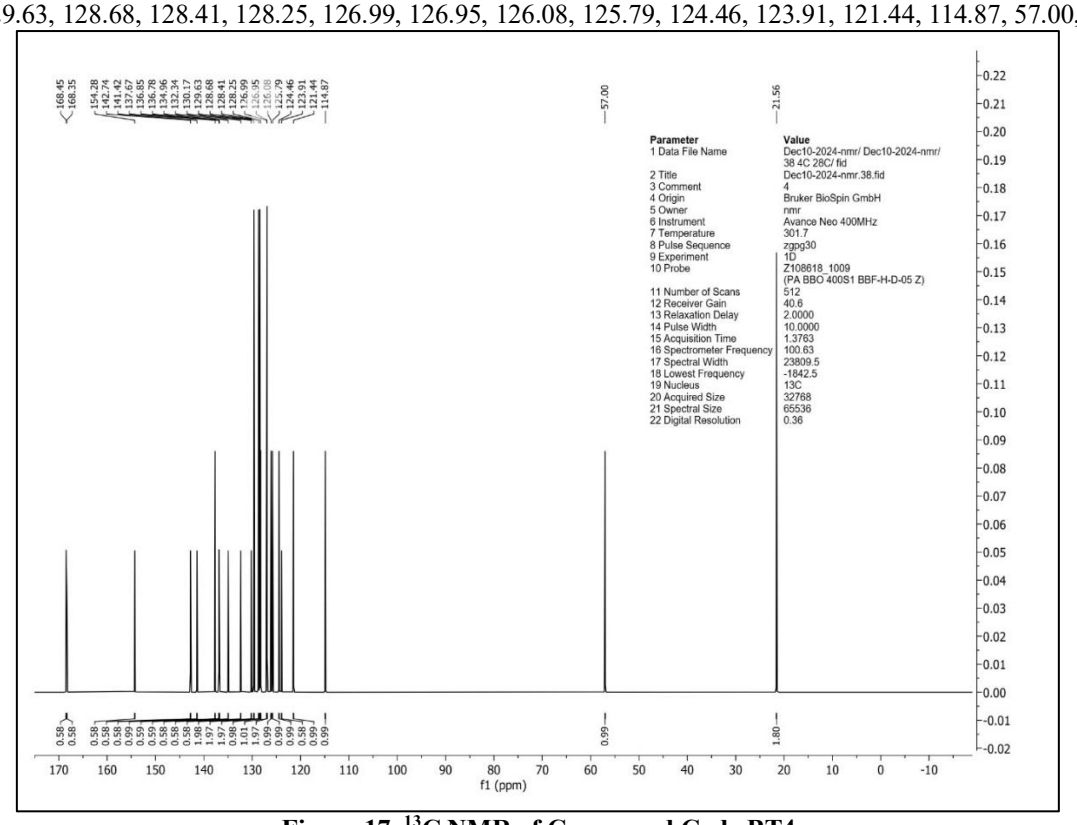

Figure 17. ^{13}C NMR of Compound Code BT4

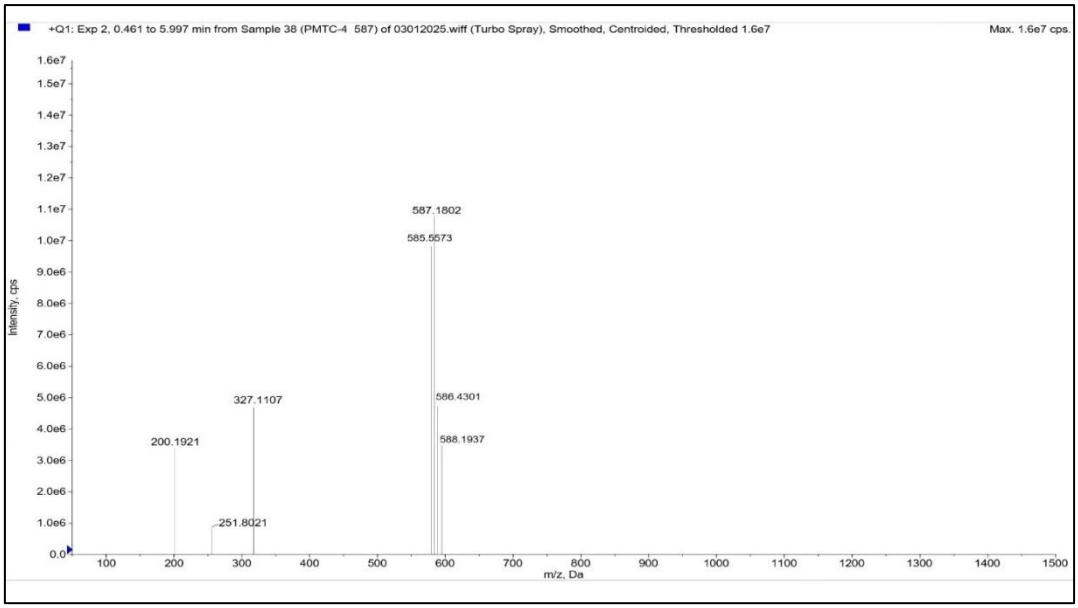

Figure 18. Mass Spectra of Compound Code BT4

3.3.4 Spectral Characterization of Compound Code CD4

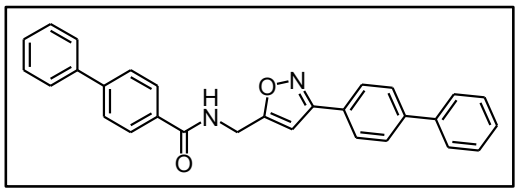

IR (KBr, cm^{-1}) 1653.07 (C=O), 3324.46 ($N\text{-}H_{str}$),1100.44 (C-O), 1520.94*(C=N)*.

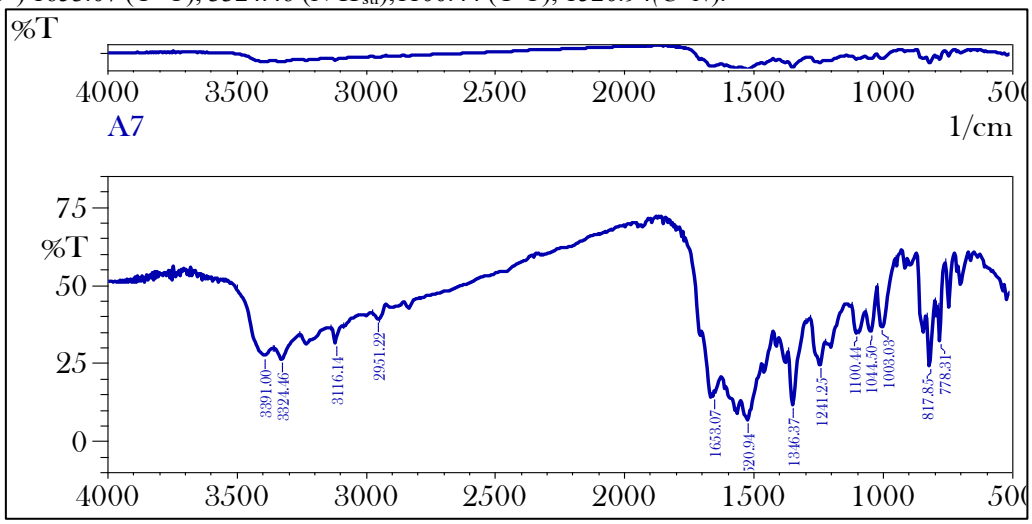

Figure 19. IR Spectra of Compound Code CD4

^{1}H NMR (500 MHz, Chloroform-*d*) δ 7.99 (t, *J* = 5.8 Hz, 0H), 7.91 – 7.86 (m, 1H), 7.67 – 7.55 (m, 4H), 7.48 – 7.41 (m, 2H), 7.41 – 7.33 (m, 1H), 4.82 (dd, *J* = 5.8, 0.8 Hz, 1H).

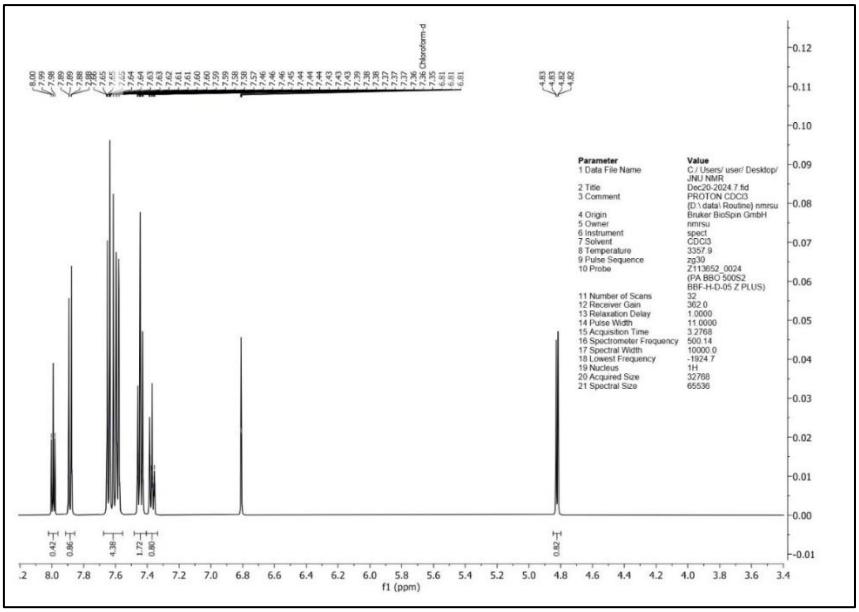

Figure 20. ^{1}H NMR Spectra of Compound Code CD4

^{13}C NMR (125 MHz, Chloroform-d) δ 168.03, 167.53, 161.22, 144.95, 141.71, 139.56, 139.49, 134.89, 131.24, 129.28, 129.20, 129.12, 128.79, 128.25, 127.98, 127.91, 127.53, 127.48, 127.40, 127.33, 127.21, 101.58, 35.97.

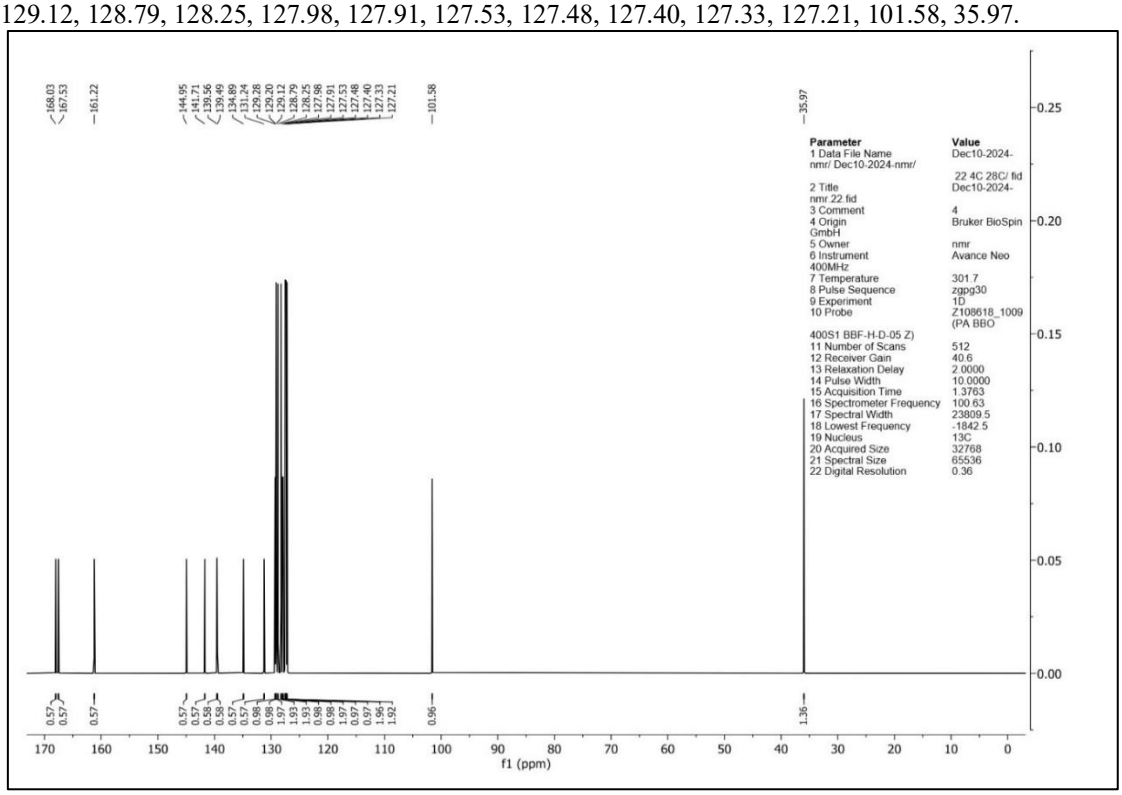

Figure 21. ^{13}C NMR Spectra of Compound Code CD4

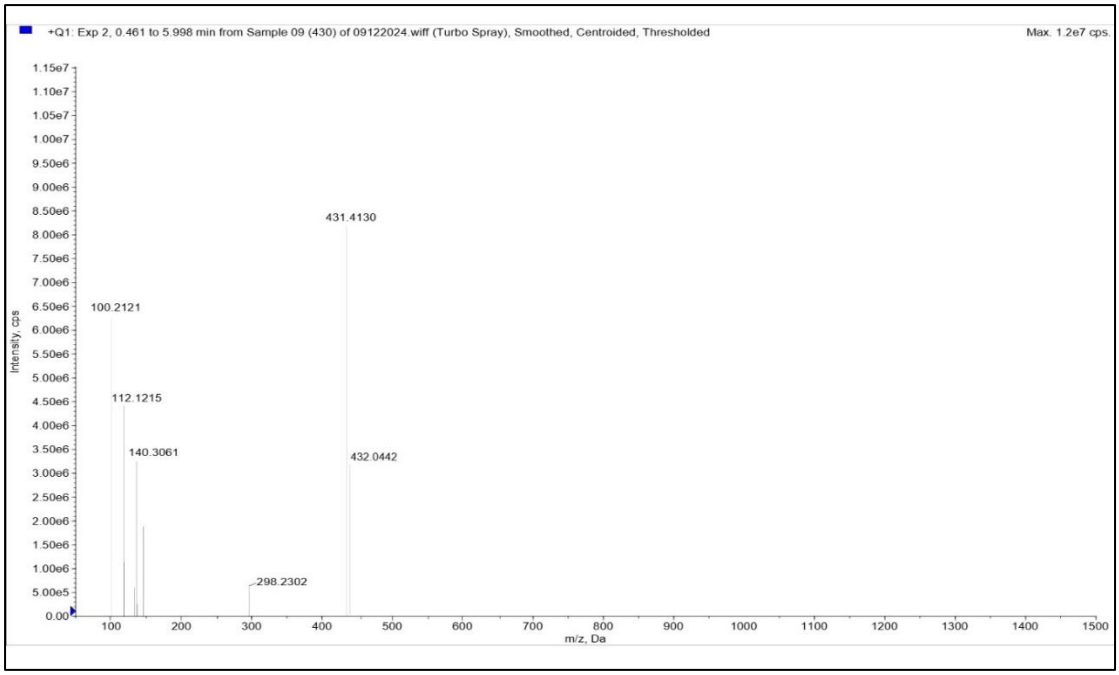

Figure 22. Mass Spectra of Compound Code CD4

3.3.5 Spectral Characterization of Compound Code CD16

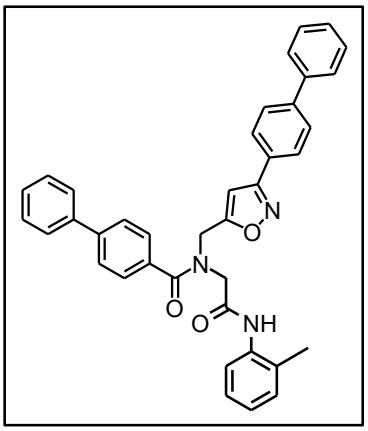

IR (KBr, cm^{-1}) 1647.28 (C=O), 3396.79 (N-H $_{str}$), 1008.81 (C-O), 1558.55 (C=N).

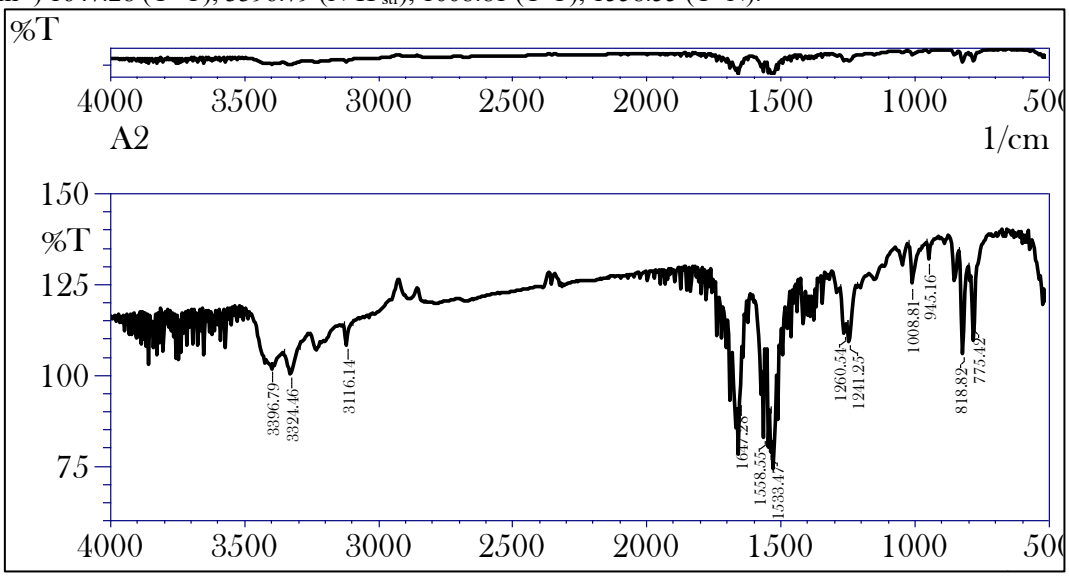

Figure 23. IR Spectra of Compound Code CD16

^{1}H NMR (500 MHz, Chloroform-*d*) δ 7.86 – 7.80 (m, 1H), 7.74 – 7.68 (m, 1H), 7.67 – 7.62 (m, 1H), 7.63 – 7.55 (m, 2H), 7.51 – 7.41 (m, 2H), 7.41 – 7.33 (m, 1H), 7.28 – 7.19 (m, 1H), 4.72 (d, *J* = 1.1 Hz, 1H), 4.11 (s, 1H).

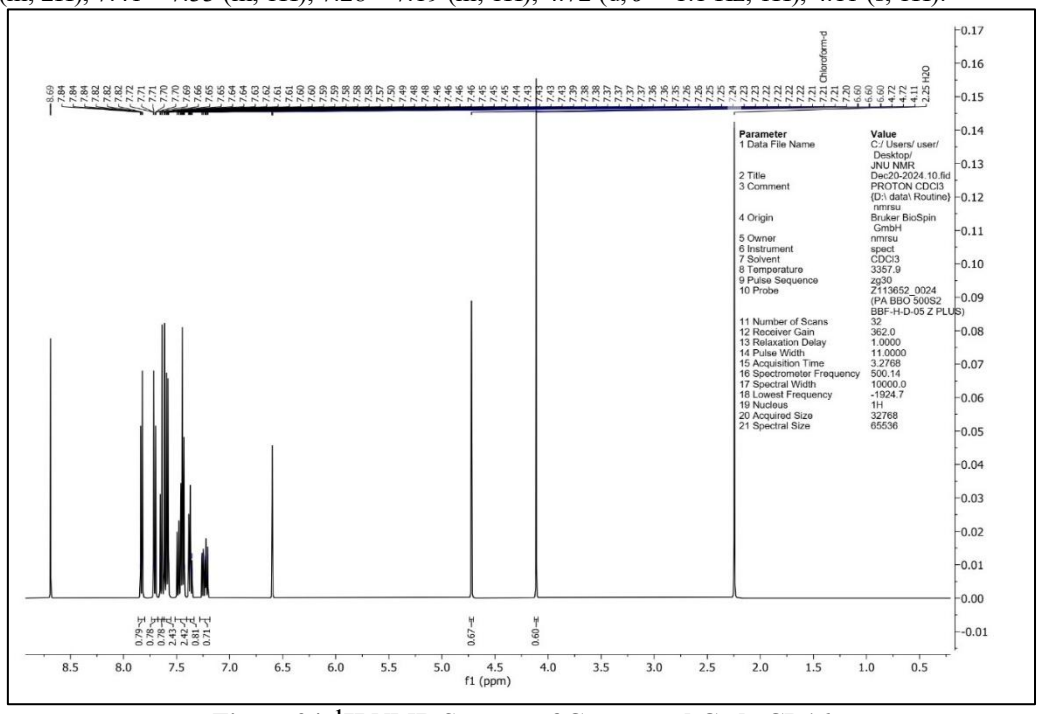

Figure 24. ^{1}H NMR Spectra of Compound Code CD16

^{13}C NMR (125 MHz, Chloroform-d) δ 170.34, 168.96, 163.28, 160.91, 145.06, 141.71, 139.56, 139.49, 137.15, 136.67, 131.42, 131.25, 130.11, 129.28, 129.20, 129.12, 128.78, 128.37, 127.98, 127.91, 127.53, 127.48, 127.40, 127.33, 127.21, 126.17, 125.13, 122.69, 101.55, 50.78, 44.47, 17.87.

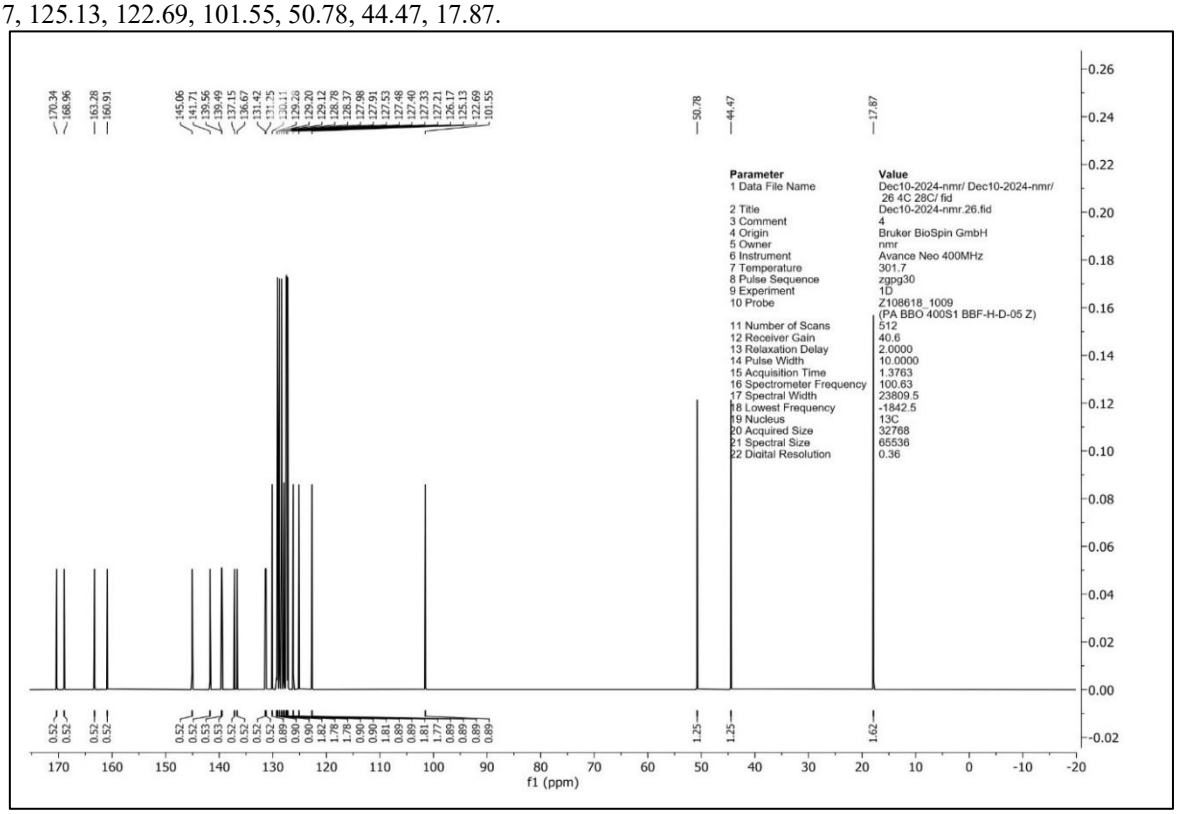

Figure 25. ^{13}C NMR Spectra of Compound Code CD16

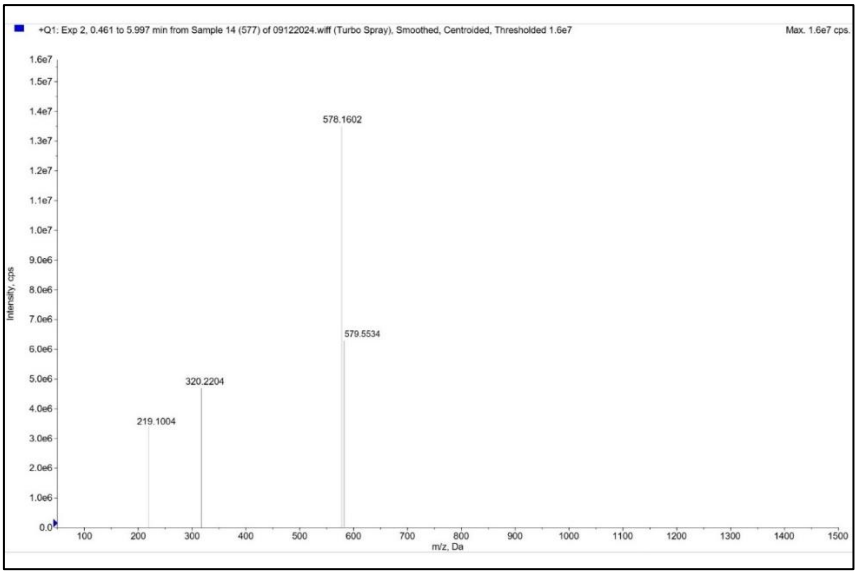

Figure 26. Mass Spectra of Compound Code CD16

3.3.6 Spectral Characterization of Compound Code CD22

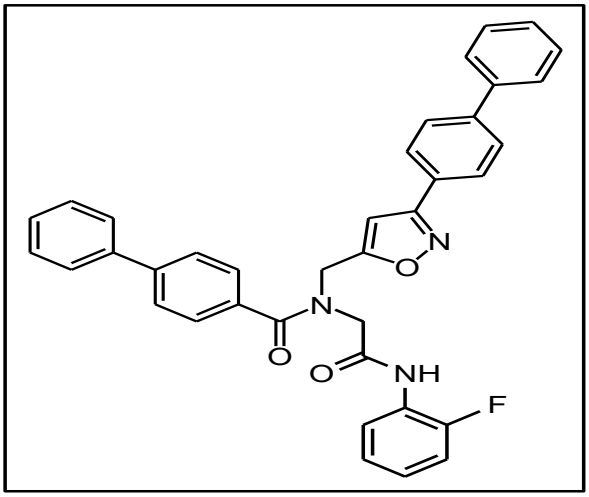

IR (KBr, cm^{-1}) 1640.53 (C=O), 3277.20 (N-H $_{str}$) 1044.50 (C–O_{str}) 1595.20 (C=N), 1256.36 (C-F), 1000 and 1360

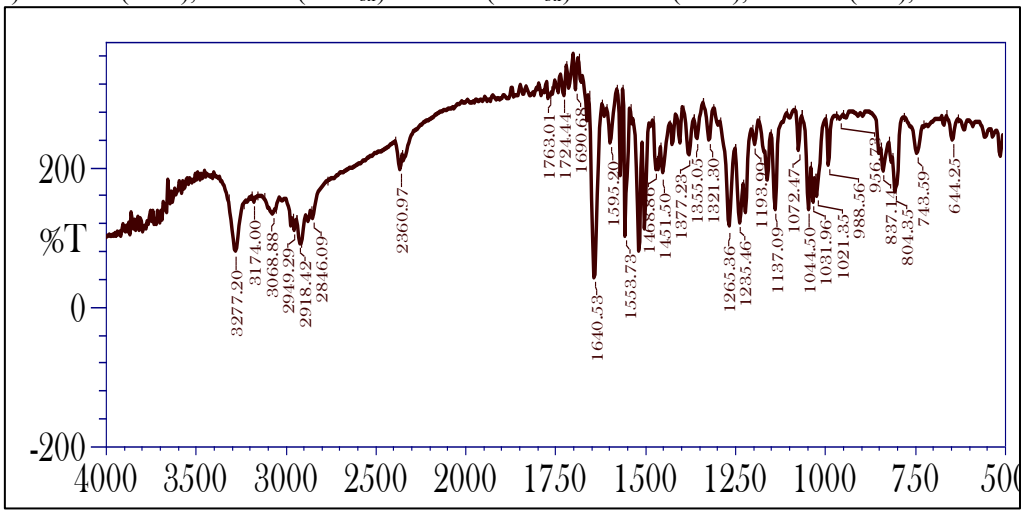

Figure 27. IR Spectra of Compound Code CD22

^{1}H NMR (500 MHz, Chloroform-*d*) δ 9.28 (d, *J* = 3.3 Hz, 0H), 7.86 – 7.80 (m, 1H), 7.74 – 7.68 (m, 1H), 7.67 – 7.55 (m, 4H), 7.48 – 7.41 (m, 1H), 7.41 – 7.33 (m, 1H), 7.24 (ddd, *J* = 9.0, 8.2, 1.5 Hz, 0H), 7.16 (ddd, *J* = 10.1, 7.9, 1.4 Hz, 0H), 7.07 (tdd, *J* = 8.2, 4.0, 1.5 Hz, 0H), 6.60 (d, *J* = 1.0 Hz, 0H), 4.72 (d, *J* = 1.1 Hz, 1H), 4.11 (s, 1H).

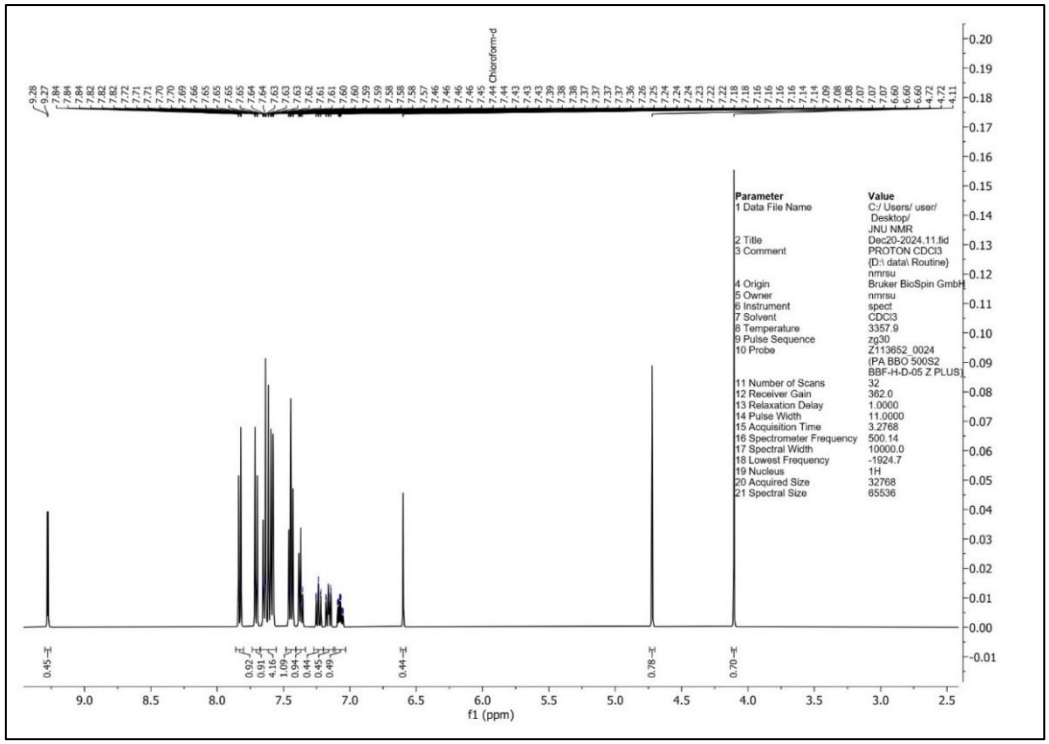

Figure 28. ^{1}H NMR Spectra of Compound Code CD22

^{13}C NMR (125 MHz, Chloroform-d) δ 168.84, 168.67, 154.30, 151.18, 139.87, 136.83, 136.35, 135.87, 134.62, 131.76, 130.53, 128.77, 128.75, 128.40, 128.24, 127.79, 127.34, 126.47, 124.30, 121.93, 119.82, 118.55, 110.77, 57.69, 47.41.

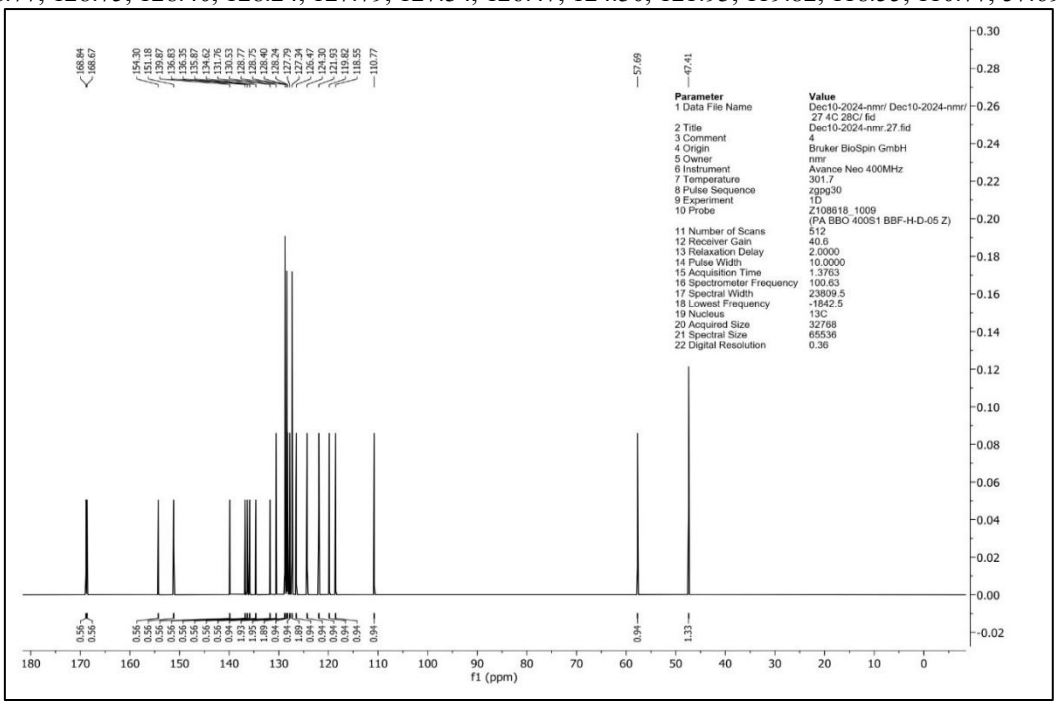

Figure 29. ^{13}C NMR Spectra of Compound Code CD22

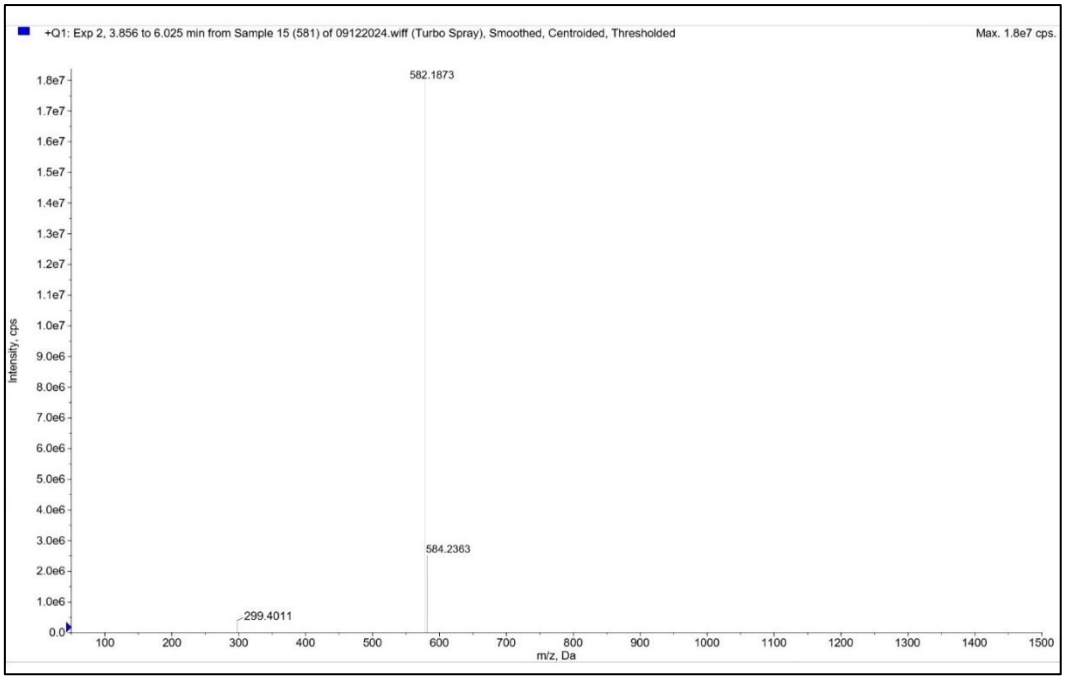

Figure 30. Mass Spectra of Compound Code CD22

3.4 In-Vivo Evaluation of Anti-Inflammatory Activity

All six synthesized compounds represented measurable anti-inflammatory effects with varying degrees of edema inhibition. The doses selection based on *in-silico* LD_{50} prediction ensued that the administered concentrations were safe and non-toxic, as no behavioural and physiological abnormalities were observed in any treated group.

3.4.1 *In-silico* Evaluation of Acute Oral Toxicity (LD_{50})

Acute oral toxicity evaluation results (Table 3 and Figure 31) reveal distinct differences in the LD_{50} results of the evaluated test materials. The material with the highest LD_{50} of any of the tested materials is MB3; therefore, MB3 exhibited the least toxicity of all tested materials. The tested material with the lowest LD_{50} is BT4; therefore, BT4 exhibited the most toxicity of all tested materials. The LD_{50} for CD4, CD22, CD16, and FB5 indicated moderate toxicity compared to the other evaluative test materials. The rank order of LD_{50} toxicities is as follows: MB3 > CD4 > CD22 > CD16 > FB5 > BT4.

Table 3. *In-silico* Assessment of Acute Oral Toxicity (LD_{50})

Compound Code	LD_{50} (mg/kg, Oral)	Toxicity Category (GHS)	Significance Interpretation
BT4	400	Category 4	Most toxic
FB5	800	Category 4	Moderately toxic
CD16	850	Category 4	Moderately toxic
CD22	1350	Category 4-5	Mild toxicity
CD4	1600	Category 5	Mild toxicity
MB3	2300	Category 5	Least toxic

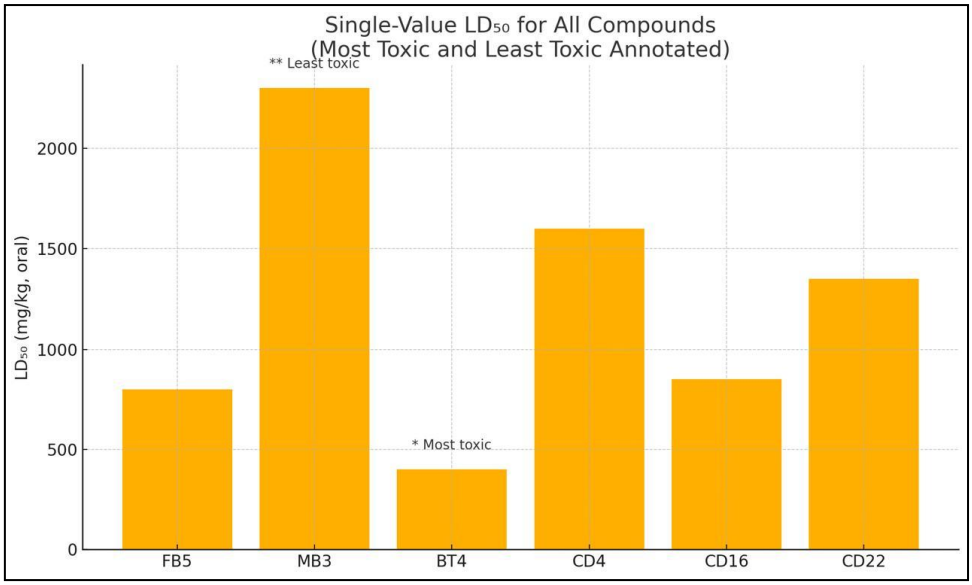

Figure 31: *In-silico* Assessment of Acute Oral Toxicity (LD_{50})

3.4.2 Effect of Treatments on Paw Edema Volume

The paw edema volume (mean ± SEM) for Group A (Table 4 and Figure 33-32) consistently indicated ongoing high levels of inflammation through the study. The other treated groups (Groups B-H) indicated substantially reduced levels of swelling when compared to Group A at each timepoint ($p < 0.001$). Among the tested derivatives FB5 (Group G) and CD16 (Group F) exhibited the highest anti-inflammatory activity, showing inhibition values comparable to the standard drug (Group H) at the 5-hour mark. Compound FB5 produced the most pronounced reduction in paw edema, indicating strong suppression of carrageenan-induced inflammatory mediators. CD16 also displayed robust and consistent inhibition across all time points, suggesting favourable pharmacodynamic behaviour. In contrast, compounds BT4, MB3, CD22, and CD4 (Group B-E) produced moderate to mild responses. A significant time-dependent decrease in swelling was attained with all treated groups; therefore, confirming the effectiveness of their anti-inflammatory effect.

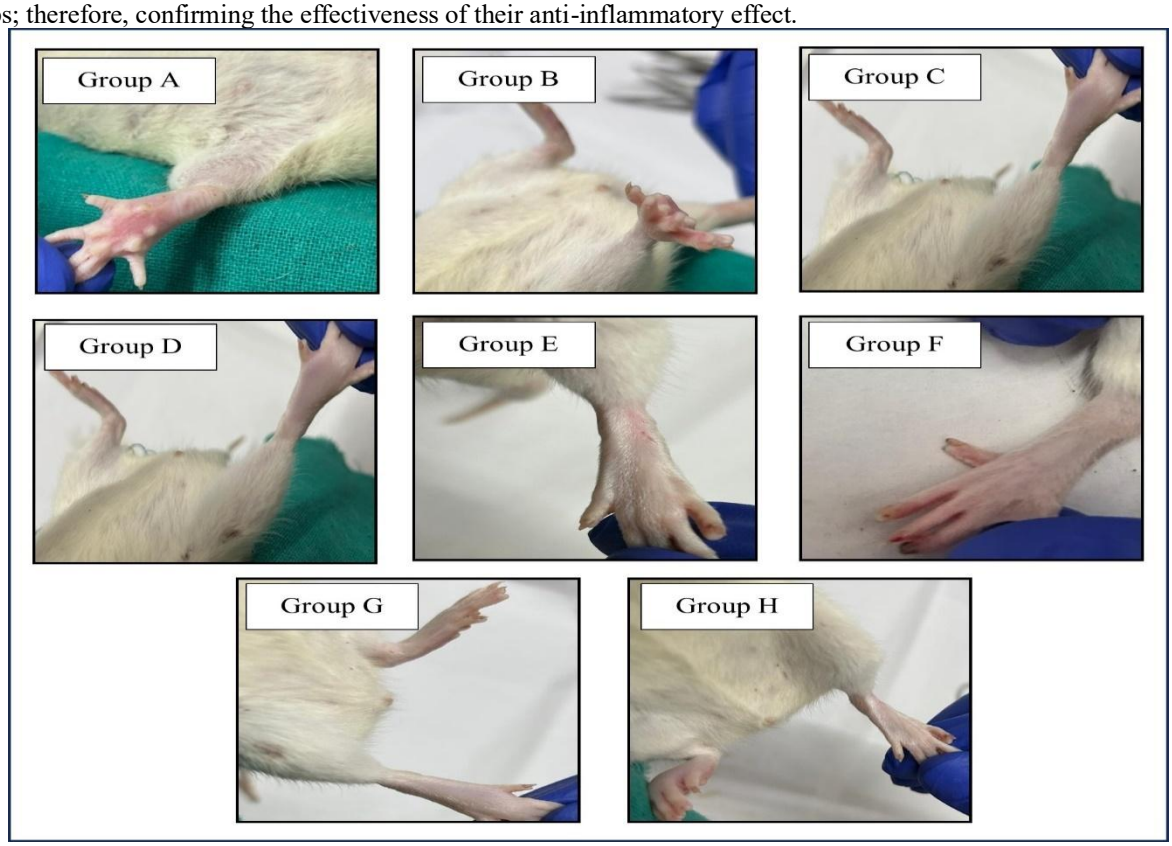

Figure 32: Anti-inflammatory Activity of Synthesized Compound in Carrageenan Induced Paw Edema

Table 4: Effect of Synthesized Compounds on Carrageenan Induced Paw Edema in Rat

Groups	Paw Edema Volume (ml)									
	1h		2h		3h		4h		5h	
	Mean	SD	Mean	SD	Mean	SD	Mean	SD	Mean	SD
Group A (Carageenan)	1.73	0.015	1.79	0.014	1.84	0.014	1.88	0.010	1.93	0.010
Group B (BT4)	1.69	0.019	1.66	0.014	1.63	0.014	1.6	0.014	1.57	0.014
Group C (MB3)	1.66	0.019	1.63	0.019	1.60	0.019	1.57	0.019	1.54	0.019
Group D (CD22)	1.65	0.019	1.62	0.019	1.59	0.019	1.53	0.019	1.53	0.019
Group E (CD4)	1.64	0.019	1.61	0.019	1.58	0.019	1.55	0.019	1.52	0.019
Group F (CD16)	1.60	0.010	1.56	0.010	1.52	0.010	1.48	0.010	1.44	0.010
Group G (FB5)	1.57	0.010	1.53	0.010	1.49	0.010	1.45	0.010	1.41	0.010
Group H (Diclofenac 10mg/kg/bw)	1.50	0.008	1.46	0.008	1.42	0.008	1.38	0.008	1.34	0.008

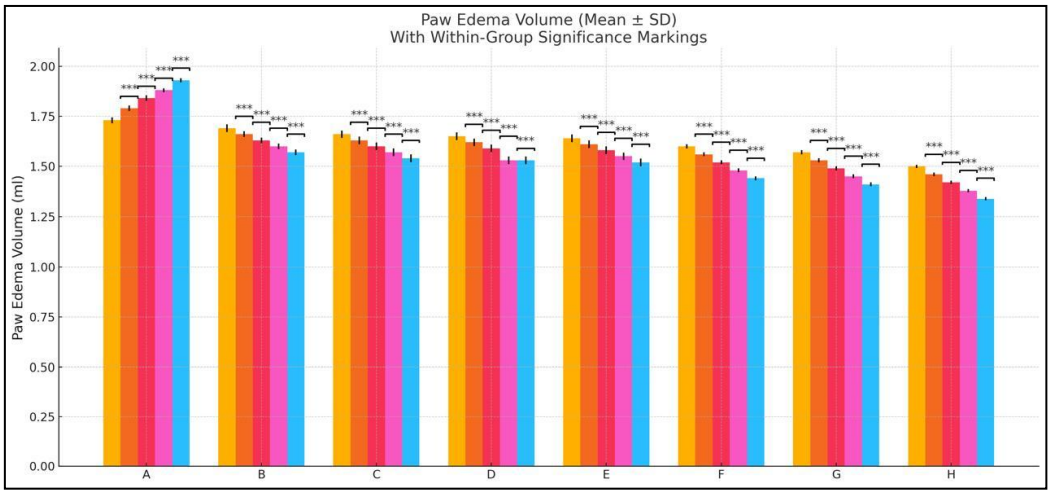

Figure 33: Effect of Treatments on Paw Edema Volume of Synthesized Compounds and Carrageenan Treated Rats

3.4.3 Percentage Inhibition of Paw Edema

The percentage of inhibition of paw edema (mean ± SEM) increased with time from treatment for all treated groups (Table 5 and Figure 34). The time-dependent percentage inhibition of paw edema for six synthesized compounds compared with the standard drug diclofenac (Group H). Among the test compound, FB5 (Group G) and CD16 (Group F) represented the highest anti-inflammatory activity, reaching 27.01% and 25.45% inhibition at 5 hours, respectively. Moderate activity was observed with BT4, MB3, CD22, and CD4 (Group B-E) showed comparatively lower inhibition. Diclofenac produced the greatest effect (30.49%) which validated the experiment. Each of the groups showed statistically significant increases in the percentage inhibition over each successive hour (1 to 2 hours) (2 to 3 hours) (3 to 4 hours) (4 to 5 hours) demonstrating sustained anti-inflammatory effects (Figure 34).

Table 5: Inhibition of Paw Edema in Synthesized Compounds and Carrageenan Treated Rats

Groups	% Inhibition of Paw Edema					
	1h	2h	3h	4h	5h	6h
Group B (BT4)	2.49	7.26	11.41	15.03	18.44	2.49
Group C (MB3)	4.22	9.22	13.32	16.89	20.26	4.22
Group D (CD22)	4.8	9.78	13.86	17.42	20.78	4.8
Group E (CD4)	5.38	10.34	14.4	17.95	21.3	5.38
Group F (CD16)	7.7	13.13	17.66	21.67	25.45	7.7

Group G (FB5)	9.43	14.8	19.29	23.26	27.01	9.43
Group H (Diclofenac 10mg/kg)	13.31	18.55	22.93	26.82	30.49	13.31

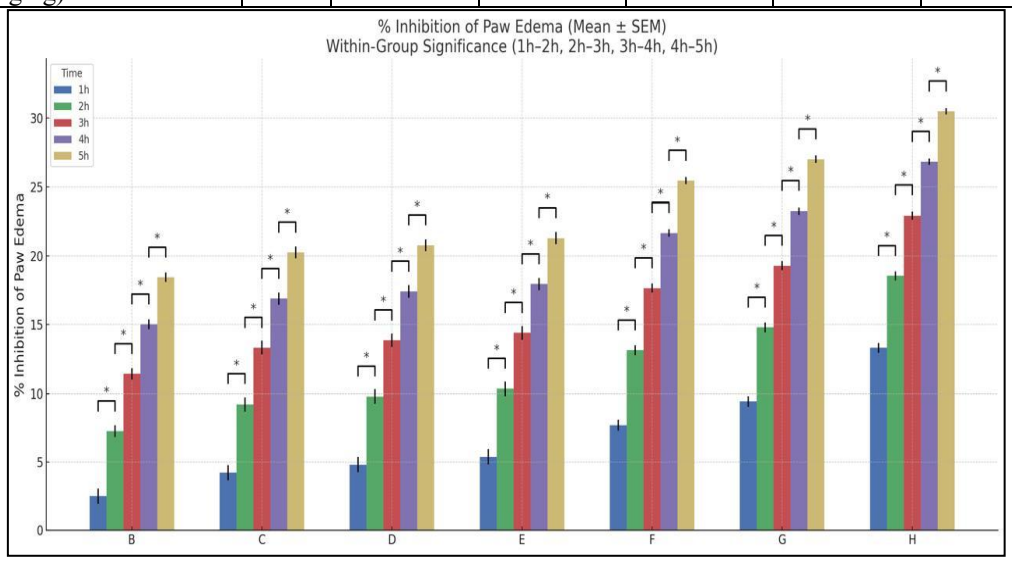

Figure 34: Inhibition of Paw Edema Volume in Synthesized Compounds and Carrageenan Treated Rats

3.4.4 Histopathological Evaluation of Paw Tissue

Histopathological examination of paw tissues revealed that there were significant differences between experimental groups regarding inflammatory pathology (Figure 35); Group A's tissue sections exhibited severe pathological change due to the presence of a great number of inflammatory cells, evidence of pronounced edema, synovial hyperplasia and the loss of normal tissue architecture, thereby exhibiting prolonged inflammatory response. On the other hand, paw tissues from treated groups presented with differing levels of histological protection. Groups B to E presented with moderate decreases in the degree of inflammatory infiltrates and edema; however, all groups presented with low levels of synovial hyperplasia. In particular, Groups F, G and H presented with significant restoration of their normal tissue architecture with very few inflammatory cells and limited edema. Histopathological study revealed that sub-plantar injection of carrageenan leads higher cellular infiltrates whereas synthesized compounds and standard drug treated rats showed less cellular infiltrates as compared to carrageenan treated rats.

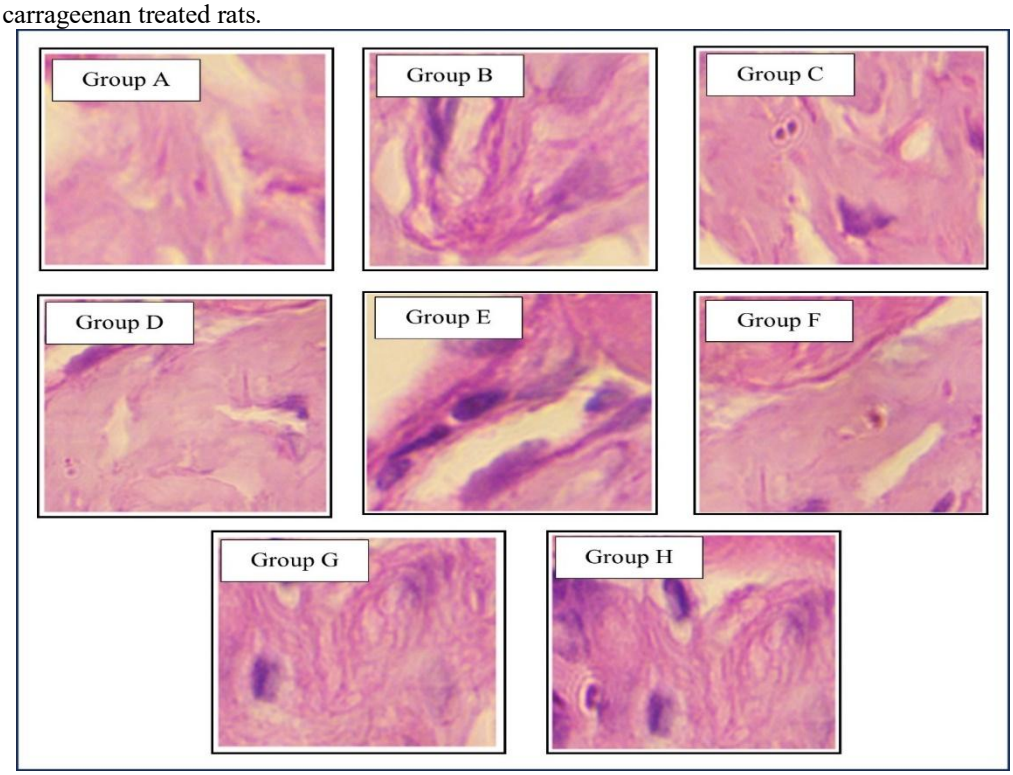

Figure 35: Histological Changes in Paw Edema after Injection of Carrageenan and Synthesized Compounds Treated Rats with 10x Magnification (Arrows Indicates the Infiltrated Cells)

3.5 DISCUSSION

The present study successfully designed, synthesized and evaluated a new series of benzimidazole and isoxazole derivatives, demonstrating promising anti-inflammatory potential. Molecular docking analysis revealed that the selected compound (Code; MB3, FB5, BT4, CD4, CD16 and CD22) exhibited a strong binding affinity towards the protein target (PDB ID: 1Q7A), surpassing the reference drug diclofenac in several cases, thus validating their structural suitability for anti-inflammatory activity. Among these, Fb5, CD16 and MB3 displayed the most favorable docking scores supported by key hydrogen-bonding and hydrophobic interaction within the enzymes active site.

The structural integrity of the synthesized compounds was confirmed through comprehensive analysis. IR spectra verified the presence of key functional groups, including carbonyl, imine, sulfonyl and halogen-specific bands. The ^{1}H and ^{13}C NMR data further supported the proposed molecular frameworks by displaying characteristic aromatic, aliphatic and heterocyclic signals consistent with each derivative. Mass spectrometry provided molecular ion peas matching calculated masses, which validating successful synthesis and purity of six synthesized compounds (MB3, FB5, BT4, CD4, CD16 and CD22).

The in-vivo carrageenan-induced paw edema model further confirmed the pharmacological relevance of these findings. Compounds FB5 and CD16 showed the highest percentage inhibition of edema, approaching the activity of diclofenac at the 5h mark, indicating strong suppression of inflammatory mediators. Other derivatives like BT4, MB3, CD4 and CD22, produced moderate yet significant anti-inflammatory effects, suggesting that structural variations influence pharmacodynamic behavior.

Toxicity prediction indicated that all compounds all within an acceptable safety margin, with MB3 exhibiting the least toxicity and BT4 the highest. Histopathological evaluation supported these outcomes, showing reduced inflammatory cell infiltration and tissue restoration in treated groups compared to the control.

3.6 CONCLUSION

The study successfully designed, synthesized and evaluated novel benzimidazole and isoxazole derivatives with significant anti-inflammatory activity. Molecular docking and spectral characterization confirmed their structural integrity and strong interaction to targeted protein (PDB ID: 1Q7A). The in-vivo findings demonstrated that compound FB5 and CD16 produced the highest anti-inflammatory action, comparable to the standard drug (diclofenac sodium), while other derivatives showed acceptable safety margins. This research work represented the promising lead molecules for further optimization and development of safer anti-inflammatory agents..

REFERENCE

1. Stone WL, Basit H, Zubair M, Burns B. Pathology, inflammation. InStatPearls [Internet] 2024 Aug 11. StatPearls Publishing.

2. Calhelha RC, Haddad H, Ribeiro L, Heleno SA, Carocho M, Barros L. Inflammation: what's there and what's new?. Applied Sciences. 2023 Feb 10;13(4):2312.

3. Chen L, Deng H, Cui H, Fang J, Zuo Z, Deng J, Li Y, Wang X, Zhao L. Inflammatory responses and inflammation-associated diseases in organs. Oncotarget. 2017 Dec 14;9(6):7204.

4. Al-Saeed A. Gastrointestinal and cardiovascular risk of nonsteroidal anti-inflammatory drugs. Oman medical journal. 2011 Nov;26(6):385.

5. Kabir E, Uzzaman M. A review on biological and medicinal impact of heterocyclic compounds. Results in Chemistry. 2022 Jan 1;4:100606.

6. Zielińska A, Karczewski J, Eder P, Kolanowski T, Szalata M, Wielgus K, Szalata M, Kim D, Shin SR, Słomski R, Souto EB. Scaffolds for drug delivery and tissue engineering: The role of genetics. Journal of Controlled Release. 2023 Jul 1;359:207-23.

7. Mahurkar ND, Gawhale ND, Lokhande MN, Uke SJ, Kodape MM. Benzimidazole: A versatile scaffold for drug discovery and beyond–A comprehensive review of synthetic approaches and recent advancements in medicinal chemistry. Results in Chemistry. 2023 Dec 1;6:101139.

8. Sahoo BM, Kumar BV, Panda KC, Banik BK, Tiwari A, Tiwari V, Singh S, Kumar M. Isoxazole Derivatives as Potential Pharmacophore for New Drug Development. InFrontiers in Medicinal Chemistry: Volume 10 2023 Oct 26 (pp. 1-49). Bentham Science Publishers.

9. Gontijo VS, Viegas FP, Ortiz CJ, de Freitas Silva M, Damasio CM, Rosa MC, Campos TG, Couto DS, Tranches Dias KS, Viegas C. Molecular hybridization as a tool in the design of multi-target directed drug candidates for neurodegenerative diseases. Current neuropharmacology. 2020 May 1;18(5):348-407.

10. Choudhary S, Arora M, Verma H, Kumar M, Silakari O. Benzimidazole based hybrids against complex diseases: A catalogue of the SAR profile. European Journal of Pharmacology. 2021 May 15;899:174027.

11. Ahmadi A. Synthesis, characterization and biological evaluation of some novel Benzimidazole derivatives. Bulgarian Chemical Comm. 2014 Jan 1;46(2):245-52.

12. Britton D, Noland WE, Pinnow MJ, Young Jr VG. Crystal packing: an examination of the packing of molecules approximately isosteric with 4, 5-dichlorophthalic anhydride. Helvetica chimica acta. 2003 Apr;86(4):1175-92.

13. Kadhim AJ. Synthesis and characterization benzimidazole ring by using o-phenylinediamine with different compounds and using Mannich reaction for preparation of some derivatives. Oriental Journal of Chemistry. 2018 Jan 1;34(1):473-81.

14. Morgan KJ, Turner AM. Studies in heterocyclic chemistry—III: The mechanism of formation of

**Author for Correspondence: dean_pharma@iimtindia.net, shabena.pharma@gmail.com.*

benzimidazoles from o-amino anilides. Tetrahedron. 1969 Jan 1;25(4):915-27.
15. Kulkarni P. An efficient solvent-free synthesis of 3, 4-disubstituted isoxazole-5 (4H)-ones using microwave irradiation. Journal of the Indian Chemical Society. 2021 Jan 1;98(1):100013.
16. Saini RK, Joshi YC, Joshi P. Synthesis of novel isoxazole derivatives from 1, 3-diketone derivatives. Heterocyclic Communications. 2007 Aug;13(4):219-22.
17. Rao HS, Senthilkumar SP. A convenient procedure for the synthesis of allyl and benzyl ethers from alcohols and phenols. Journal of Chemical Sciences. 2001 Jun;113(3):191-6.
18. Mallik NN, Manasa C, Basavanna V, Shanthakumar DC, Ningaiah S, Lingegowda NS. Synthesis of fused isoxazoles: A comprehensive review. Engineering Proceedings. 2024 Jan 30;59(1):222.
19. Fischer MJ. Amine coupling through EDC/NHS: a practical approach. InSurface plasmon resonance: methods and protocols 2010 Jan 22 (pp. 55-73). Totowa, NJ: Humana Press.
20. Mahmoud KA, Long YT, Schatte G, Kraatz HB. Rearrangement of the active ester intermediate during HOBt/EDC amide coupling. European journal of inorganic chemistry. 2005 Jan;2005(1):173-80.
21. Procopio D, Siciliano C, Di Gioia ML. Reactive deep eutectic solvents for EDC-mediated amide synthesis. Organic & Biomolecular Chemistry. 2024;22(7):1400-8.
22. Ismail SM, Rao KR, Bhaskar M. Evaluation of anti-inflammatory activity of Boswellia serrata on carrageenan induced paw edema in albino Wistar rats. Int. J. Res. Med. Sci. 2016 Jul;4(7):2980-6.
.